2,3,7,8-Tetrachlorodibenzo-*p*-dioxin (TCDD) and early human pancreatic development

By

Erin M. MacFarlane

B.Sc. (Hons) 2017 Carleton University

A thesis submitted to the Faculty of Graduate and Postdoctoral Affairs in partial fulfillment of the requirements for the degree of

Master of Science

in

Biology

Carleton University
Ottawa, Ontario

Abstract

Environmental factors such as pollutants are associated with diabetes incidence. Of particular interest is exposure to persistent organic pollutants (POPs) during critical stages of fetal development. TCDD (2,3,7,8-tetrachlorodibenzo-*p*-dioxin) is a potent ligand of the aryl hydrocarbon receptor, which leads to induction of cytochrome P450 (CYP) 1A1 enzymes. We hypothesize that POPs such as TCDD accumulate in the pancreas, thereby eliciting stress on developing beta cells through induction of CYP1A1. Here, I exposed rodent alpha and beta cell lines to TCDD *in vitro,* but did not observe induction of *Cyp1a1* gene expression or enzyme activity, meaning that this pathway is not activated in immortalized pancreatic endocrine cell lines. I also differentiated human embryonic stem cells toward pancreatic cell fate *in vitro* to study how TCDD exposure impacts human beta cell development. I concluded that TCDD might impede normal development of beta cells, potentially through induction of *CYP1A1* and other embryonic lineages.

Acknowledgements

I would firstly like to acknowledge my supervisor, Dr. Jenny Bruin, for her support and guidance throughout my project, on-going patience and understanding toward the struggles of stem cell culture, and encouragement through my endless troubleshooting. Thank you to the rest of the Bruin lab members, particularly Kayleigh Rick and Myriam Hoyeck, for occasional scientific support and frequent emotional support. This venture would have been much less enriching without you.

I also extend thanks to my committee members, Dr. Iain McKinnell and Dr. Jan Mennigen, for helpful suggestions and guidance during my degree. An honourable mention also goes to Dr. Bruce McKay, who generously allowed me to use his flow cytometer over the course of my project.

Lastly, thank you to my family for dealing with my frustrations, wins, and losses over the past two years. Although they didn't quite understand my day-to-day life in research, they continue to be a source of unwavering encouragement. Thank you to Andrew for coming to the lab with me on weekends, for letting me cry about my failed experiments, and celebrating my successes with me.

Dedicated to every woman in science.

Table of Contents

List of Tables

List of Figures

List of Appendices

Introduction

Thesis Overview

Genetics and lifestyle both play a well-established role in the pathogenesis of diabetes, however environmental factors are also of interest as a third contributing cause. During pancreatic development, the formation of healthy and functional beta cells is critical for insulin production, and thus blood glucose regulation after birth. Unlike other types of cells in the body, such as the liver, beta cells in adults have very low replication rates. This suggests that the beta cell reservoir cultivated during fetal development is largely what an individual relies on for the duration of their life. We therefore hypothesize that biochemical disturbances in the environment of the developing fetus – a time when the cells are particularly vulnerable to damage – may result in beta cell loss or dysfunction.

Exposure to persistent organic pollutants (POPs) increase lifetime risk of developing diabetes (Persky *et al*., 2012; Lee *et al*., 2010; Codru *et al*., 2007; Kang et al., 2006; Bertazzi *et al*., 1998; Henriksen *et al*., 1997). Dioxins and dioxin-like compounds are examples of POPs that activate the aryl hydrocarbon receptor (AhR) pathway, resulting in increased production of cytochrome P450 (CYP) enzymes and associated harmful by-products. The goal of my project is to investigate the impact of 2,3,7,8-tetrachlorodibenzo-*p*-dioxin (TCDD) – the most potent dioxin – on pancreas development via differentiation of human embryonic stem cells toward insulin-producing pancreatic beta cells. This will provide insight into how environmental pollutants may play a role in the dysfunction of pancreatic

beta cells, and ultimately diabetes risk, especially during critical early stages of fetal development.

Diabetes: A brief introduction

Diabetes is a metabolic disorder that is characterized by chronic, poor glycemic control resulting in a wide range of systemic symptoms and complications such as increased risk of infection, limb amputations, and cardiovascular disease. Diabetes prevalence is increasing worldwide, and is projected to afflict one in ten adults by 2040 (International Diabetes Foundation, 2017). Type 1 diabetes (T1D), commonly known as adolescent diabetes, is caused by an autoimmune attack against pancreatic beta cells leading to a loss of functional insulin-producing cells. Individuals with T1D require multiple daily insulin injections to regulate their blood glucose levels. Type 2 diabetes (T2D) results from a loss of functional beta cells in addition to peripheral insulin resistance, and accounts for approximately 90% of all cases of diabetes (International Diabetes Foundation, 2017). These patients are treated with drugs such as metformin to decrease endogenous glucose production, in addition to lifestyle changes (e.g. exercise, dietary changes, weight loss).

Diabetes has also been associated with a significant risk of developing various cancers such as cancer of the pancreas, liver, and colon (Ballotari *et al*., 2017). Diabetes is a complex metabolic disease that has been linked to various risk factors – lifestyle, genetics, and more recently environmental pollutants. In this thesis I investigate a possible pathway for pancreatic beta cell damage leading to dysfunction.

Pancreatic islets and beta cells

The endocrine pancreas is comprised of clusters of hormone-secreting cells, called the Islets of Langerhans. The two most abundant cell types, alpha cells and beta cells, work synergistically to regulate blood glucose levels. In a state of low blood glucose (e.g. between meals or while sleeping), alpha cells respond by secreting glucagon, a hormone that promotes the release of glucose via glycogenolysis. In contrast, following an increase in blood glucose (e.g. immediately after a meal), the beta cells release insulin, which binds to membrane receptors on target tissues and prompts the storage of glucose as glycogen (Figure A).

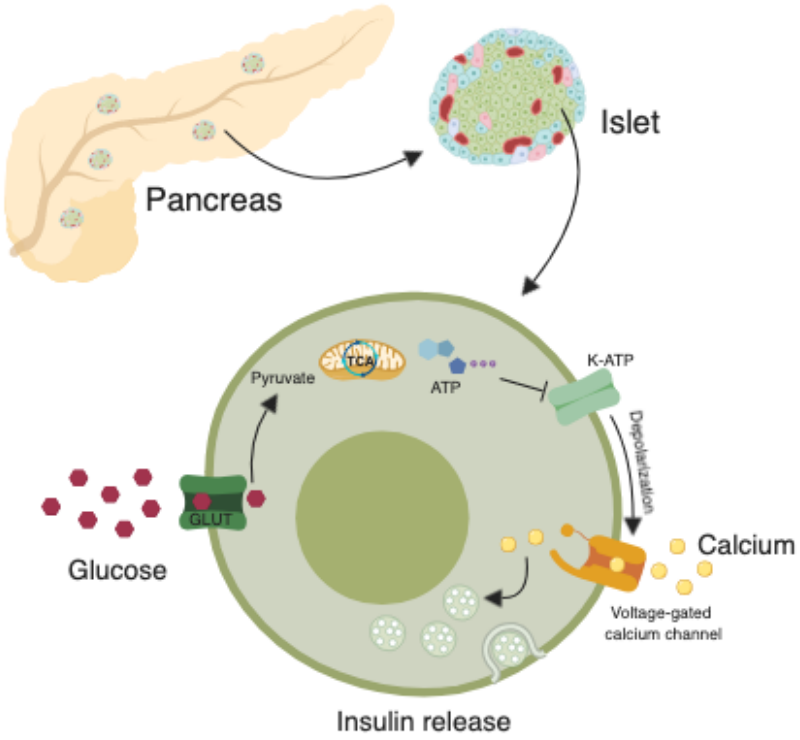

Figure A Overview of pancreatic beta cell glucose-stimulated insulin secretion (created with BioRender.com).

Other cells types within the islets contribute to systemic energy homeostasis by producing and secreting peptide hormones. Somatostatin, for example, is released by delta cells and can inhibit hormone release from alpha (glucagon) and beta (insulin) cells. Similarly, pancreatic polypeptide (produced by aptly named PP cells) can also stop the release of glucagon by alpha cells. Interestingly, ghrelin (commonly known as the 'hunger hormone') is released by cells in both the islets and the gastrointestinal tract, and has important roles in the nervous system (Xavier, 2018). Ghrelin signals hunger, prompting us to consume food and raise blood glucose levels; it also suppresses insulin secretion, thereby inhibiting glucose storage prior to food consumption. **It is important to note that islets function as a whole, and that appropriate development and organization of each cell type is necessary for efficient energy homeostasis.**

Persistent organic pollutants (POPs) and diabetes

Every day humans are exposed to numerous pollutants that have become omnipresent in our environment, intentional or otherwise. Despite their decrease or total ban in agriculture, many persistent organic pollutants (POPs) reside in the environment, where they continue to bioaccumulate through the food chain. The primary route of exposure to environmental pollutants is through direct consumption, especially via ingestion of animal products (Ruzzin *et al*., 2010). These compounds tend to be highly lipophilic and are therefore stored in fatty tissues, such as adipose tissue, liver, and potentially the pancreas. Examples of

POPs include pesticides, polychlorinated biphenyls (PCBs), and by-products of incomplete combustion (common in industrial production of chemicals). A nested case-control study within the Coronary Artery Risk Development in Young Adults (CARDIA) cohort revealed an association between low-dose POP exposure and increased diabetes risk (Lee *et al*., 2010).

Dioxins are a class of POPs that activate the aryl hydrocarbon receptor (AhR) pathway, which results in accumulation of cytochrome P450 (CYP) enzymes and production of reactive metabolites. The most potent dioxin, TCDD, is created during the production of 1,2,3-trichloropropane and some herbicides, as well as through the burning of PCBs. Direct exposure to potent organic pollutants such as polychlorinated biphenyls (PCBs) and TCDD have been linked to increased risk of developing diabetes (Persky *et al*., 2012; Lee *et al*., 2010; Codru *et al*., 2007; Kang et al., 2006; Bertazzi *et al*., 1998; Henriksen *et al*., 1997). One of the most notable instances of widespread human exposure to TCDD was during the Vietnam War when Agent Orange, a TCDD-contaminated solution used for herbicide warfare, was sprayed across vast regions of Southeast Asia (Operation Ranch Hand). Long-term health studies of U.S. veterans involved in Operation Ranch Hand have shown an increase in abnormalities of glucose homeostasis and overall diabetes prevalence (Henriksen *et al*., 1997). Further, abnormal serum insulin levels have been measured in TCDD-exposed nondiabetic individuals, suggesting an overall link between TCDD exposure, beta cell function, and glucose metabolism (Henriksen *et al*., 1997). Another large-scale human exposure to TCDD occurred in Seveso,

Italy following an industrial accident. Observed lifetime health affects included an increase in diabetes incidence, mortality associated with cardiovascular disease, as well as an increase in gastrointestinal cancer occurrence (Bertazzi *et al*., 1998).

TCDD has also been measured in blood (background levels ≤10 pg/g in the USA) (Longnecker and Michalek, 2000), breast milk (>200 pg/g fat) (Hooper *et al*., 1999), and semen of exposed individuals (Schecter *et al*., 1996), and is known to cross the placenta (Ye *et al*., 2018; Nau *et al*., 1986). Dr. Bruin and colleagues have generated preliminary data (N=1) suggesting that the human pancreas may serve as a depot for POPs, such that that their toxic effects may have a local impact on resident cells, including pancreatic endocrine cells within the Islets of Langerhans. **We hypothesize that environmental factors may contribute to the loss of functional pancreatic beta cells, thereby playing a role in the pathogenesis of diabetes.**

Cytochrome P450 (CYP) enzymes

CYP enzymes are a family of proteins that aid in the breakdown and excretion of both endogenous (e.g. synthesis of bilirubin, breakdown of vitamins) and exogenous ('xenobiotic') compounds (e.g. drugs, toxins) (Nebert and Dalton, 2006). There are 18 CYP families, however those in CYP1 through CYP4 are responsible for xenobiotic metabolism. CYP proteins are monooxygenases that have the ability to transform compounds into bioreactive species through the incorporation of a hydroxyl group. This stage of metabolism, known as Phase I,

can yield a surplus of reactive oxygen species (ROS) that may damage surrounding tissues by forming DNA adducts, for example. Phase II involves the conjugation to polar compounds, followed by excretion, generally in the urine. Prolonged activation of CYP enzymes may lead to an imbalance in Phase I and Phase II metabolism, potentially having detrimental effects on tissues.

Of the CYP enzymes involved in xenobiotic metabolism, the CYP1A family are especially important for the processing of drugs and are known for their ability to bioactivate toxins and procarcinogens (Yueh *et al*., 2005). CYP1A enzymes are activated through the AhR pathway when a ligand is bound, thereby inducing transcription of *CYP1A* genes. Polycyclic aromatic hydrocarbons (e.g. benzo(a)pyrene found in cigarette smoke; product of charred meat) and dioxins/dioxin-like compounds (e.g. TCDD) are ligands for the AhR. Hydrophobic compounds such as TCDD are able to passively enter the cell without additional molecular machinery because they can diffuse through the lipid membranes (Figure B). Once in the cytosol, TCDD complexes with the AhR and enters the nucleus. The aryl hydrocarbon receptor nuclear translocator (ARNT) directs the AhR/TCDD complex to DNA, where it interacts with xenobiotic response elements (XREs) in the promoter regions of DNA. Transcription of a wide variety of genes occurs, however we are interested in the induction of *CYP1A* genes because of their role in metabolizing procarcinogens and production of ROS in response to xenobiotic exposure. Importantly, although TCDD activates CYP1A enzymes, it is not itself metabolized by the enzymes, thus resulting in an increase in CYP1A levels without a corresponding decrease in TCDD. Increases in

CYP1A1 expression in target tissues can therefore indicate local AhR activation by TCDD and dioxin-like ligands.

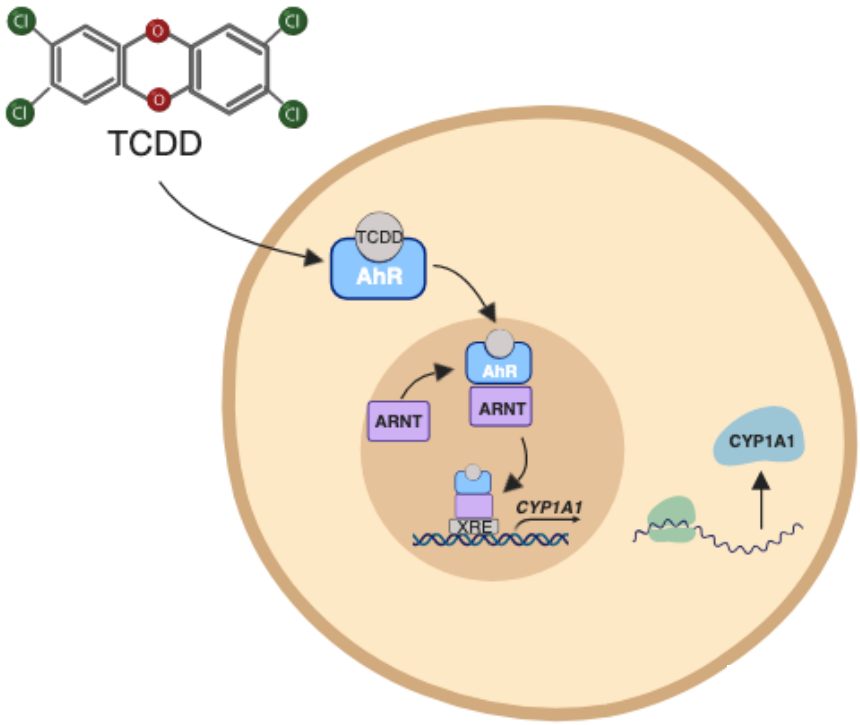

Figure B Overview of TCDD-induced activation of the aryl hydrocarbon receptor pathway and subsequent production of CYP1A1 enzymes (created with BioRender.com).

Interestingly, CYP1A1 is active in the placenta during pregnancy and is associated with various gestational complications in women who are cigarette smokers and therefore exposed to benzo(a)pyrene (Stejskalova and Pavek, 2011). The Bruin lab has shown that CYP1A1 gene expression and enzyme activity are increased in both mouse and human islets in response to direct TCDD exposure *in vitro*. Further, mice injected with either a single high dose or chronic low dose of TCDD have prolonged elevation of Cyp1a1 enzymes in their islets *in vivo*. Morphological differences in the islets have also documented

following TCDD exposure *in vivo*. **Therefore, we predict that TCDD is being stored in the pancreas and acting locally within the islets, resulting in prolonged Cyp1a1 enzyme activity, which could be a source of stress and damage.**

Human pancreas development

Human embryonic stem cells (hESCs) provide a physiologically relevant developmental model for studying the pathogenesis of disease. hESCs are derived from the inner cell mass of the blastocyst before uterine implantation and maintain pluripotent potential in culture. These cells have the ability, if given the proper environmental cues, to differentiate into each of the three germ layers, and subsequently into any cell in the human body (Xu *et al*., 2001). As outlined in Figure C, pancreas development begins with the definitive endoderm ('Stage 1'), which can be characterized by expression of transcription factors, FOXA2 and SOX17, and a cell surface marker, CXCR4. When pluripotent cells acquire definitive endoderm identity, they transiently reduce expression of transcription factors, OCT4 and SOX2 (Aksoy *et al*., 2013). The primitive gut tube then forms as a result of anterior-posterior axis definition in the definitive endoderm ('Stage 2') (Lee and Chung, 2011). As the primitive gut tube develops into the posterior foregut, expressing PDX1, it becomes biased toward pancreas and liver lineages ('Stage 3'). Pancreatic endoderm is established and characteristically co-expresses PDX1 and NKX6.1 ('Stage 4'). The pancreatic endocrine precursors are then formed, expressing PDX1, NKX6.1, NEUROD1, and NGN3, which

distinguish them from liver progenitors ('Stage 5'). Beta cell fate is established from the endocrine precursors when the cells begin co-expressing INS, PDX1, NKX6.1, and NEUROD1 ('Stage 6'). Finally, the functional, maturing beta cells express insulin, PDX1, NKX6.1, NEUROD1, and MAFA, among other key transcription factors. MAFA distinguishes the maturing beta cells from the immature beta cells and is critical for achieving glucose-responsive insulin secretion ('Stage 7').

For my project, I have been attempting to differentiate hESCs toward maturing pancreatic beta cells in a series of distinct stages that are designed to mimic critical stages of pancreas development, as in Figure C (Rezania *et al*., 2014). These stages, identified by key molecular markers, allow us to assess the impact of TCDD exposure at key points in the developmental process. Importantly, we will be able to study the immediate and downstream developmental effects of TCDD on beta cells in terms of morphology, developmental efficiency, survival, and function (insulin secretion).

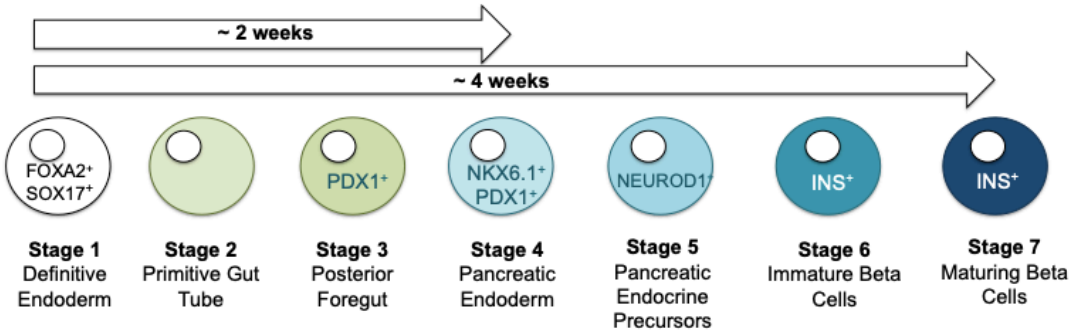

Figure C Overview of human beta cell development and associated 'Stages' of differentiation.

Summary and aims

Environmental pollutants, which are primarily introduced through the diet, serve as a potential cause for pancreatic beta cell loss and dysfunction. Exposure during fetal development via the placenta may compromise the reservoir of healthy beta cells that will help regulate glucose homeostasis later in life, thereby predisposing an individual to develop diabetes. Activation of the AhR pathway by certain pollutants, including TCDD, promotes the transcription of cytochrome P450 genes, which produce active CYP1A1 enzymes and associated harmful metabolites. We hypothesize that local induction of these enzymes in the pancreas may cause deregulation and damage within the developing islets. **Taken together, the primary goal of my project is to study the local impact of TCDD, a potent ligand for the AhR pathway and Cyp1a1 enzyme activity, on human beta cell development in vitro.**

The specific aims within my project include: **(1)** investigating if rodent beta and alpha cells lines produce Cyp1a1 gene expression and/or enzyme activity when exposed to TCDD *in vitro*; **(2)** establishing stem cell culture and differentiation protocols in the Bruin lab; and **(3)** studying how direct exposure to TCDD impacts human beta cell development using embryonic stem cell differentiation protocols.

Chapter 1: TCDD and rodent endocrine cells

1.1 Introduction and Rationale

Previous data from the Bruin Lab has shown that mouse islets produce functional Cyp1a1 enzymes following both *in vitro* and *in vivo* exposure to TCDD. The lab has also found that exposure to TCDD alters glucose homeostasis in mice. The beta cell is of particular interest because it is responsible for synthesizing and secreting insulin to help maintain glucose homeostasis, and it is the most abundant cell type in pancreatic islets. The alpha cells are the second most abundant cell type in pancreatic islets and are responsible for secreting glucagon in response to low blood glucose. Importantly, islets are clusters of various endocrine cell types that function as a whole to regulate blood glucose, therefore simply studying pancreatic islets does not provide enough insight into which cell type is specifically being affected by the TCDD. Since pancreatic beta cells are the most abundant cell type in the islet and they secrete insulin to promote glucose storage, we hypothesize that Cyp1a1 enzymes are being produced locally within the beta cells and impacting their physiology, thereby resulting in changes in glucose homeostasis.

Primary human and mouse alpha and beta cells are not highly proliferative and are therefore not amenable to tissue culture. In order to test our hypothesis, we decided to use rodent alpha-like and beta-like cell lines as a model system because we can study them in isolation, rather than as part of an entire islet. A key distinction here is that the rodent endocrine cell lines are derived from tumours or have been transfected with SV40 to induce tumourigenesis, rendering

the cell lines immortal and useful for *in vitro* studies. However this also means the cell lines are not considered true alpha or beta cells due to their proliferative properties and genetic instability as tumour cells. Contingent upon the results from the first experiments, we hoped to use one or more of the rodent cell lines as a screening tool for studying the effects of TCDD and other environmental pollutants on pancreatic endocrine cells *in vitro*.

The goal of this chapter is therefore twofold: **(1)** use rodent alpha-like and beta-like cell lines to determine in which cell type TCDD induces production of Cyp1a1 enzymes, and **(2)** to determine if any of the rodent cell lines might be suitable for studying the impact of dioxin-like pollutants *in vitro*.

1.2 Methods

Prior to experimental use, each cell line was tested for mycoplasma, a common contaminant in tissue culture, using the Lonza MycoAlert assay (#CA11006554, Lonza) according to manufacturer protocol.

Rodent beta cell lines

MIN6 and INS-1 cell lines were generously gifted by Dr. Timothy Kieffer (Vancouver, BC). MIN6 (mouse insulinoma) cells were maintained in high-glucose Dulbecco's Modified Eagle Medium (DMEM-HG) (#D5796, Sigma-Aldrich) further supplemented with 10% fetal bovine serum (FBS) (#F1051, Sigma-Aldrich) and 1 mM sodium pyruvate (#S8636, Signa-Aldrich). INS-1 (rat insulinoma) cells were cultured in Roswell Park Memorial Institute (RPMI) 1640

medium (#10-040-CV, Corning) with 10% FBS, 50 µM 2-mercaptoethanol (#M3148, Sigma-Aldrich), 10 mM HEPES (#25-060-CI, Corning), and 1 mM sodium pyruvate.

Beta-TC-6 (mouse insulinoma) cells were obtained from Dr. Michael Rudnicki (Ottawa, ON) and maintained in DMEM-HG further supplemented with 10% FBS and 1 mM sodium pyruvate. All cell lines were cultured in 10 cm tissue culture plates (#430167, Corning) and incubated at 37°C and 5% CO_2.

Rodent alpha cell lines

Alpha-TC-1 and alpha-TC-3 cells (mouse adenomas), kindly provided by Dr. Timothy Kieffer (Vancouver, BC), were cultured in DMEM-HG (#10-017-CV, Corning) further supplemented with 10% FBS and 1 mM sodium pyruvate. Cells were cultured in 10 cm tissue culture plates and incubated at 37°C and 5% CO_2.

Human liver cell line

HepG2 (human hepatocellular carcinoma) cells were kindly gifted by Dr. Timothy Kieffer (Vancouver, BC) and Dr. Bill Willmore (Ottawa, ON). HepG2 cells were maintained in DMEM-HG (#D5796, Sigma-Aldrich) further supplemented with 10% FBS and 1 mM sodium pyruvate. Cells were cultured in 10 cm tissue culture plates and incubated at 37°C and 5% CO_2.

Cyp1a1 enzyme assay

MIN6, INS-1, beta-TC-6, alpha-TC-6, alpha-TC-3, and HepG2 cells were seeded in triplicate for each treatment group at ~100,000 cells/well in a white-walled 96-well tissue culture plate (#82050-758, VWR). Cells were incubated at 37°C and 5% CO_2 for 24 hours. The following day cells were treated with complete culture media containing 10 nM TCDD (#48599, Sigma-Aldrich), DMSO vehicle control (#S276855, Sigma-Aldrich), or no additives for 48 hours. All treatments were replenished after 24 hours.

Following 48-hour treatments, media was removed and wells were rinsed with PBS (without Mg^{2+} or Ca^{2+}, PBS(-); #D8537, Sigma-Aldrich). Cyp1a1 enzyme activity was measured using Promega P450-Glo kit (#V8752, Promega), a luminescence-based assay. Cells were incubated in 1:50 luciferin-CEE substrate diluted in complete culture medium for 3 hours at 37°C and 5% CO_2, followed by the addition of 50 µL Detection Reagent and incubated for 20 minutes at room temperature in the dark. Luminescence (relative light units, RLU) was measured using a Biotek Cytation 5 plate reader.

Gene expression

MIN6, INS-1, beta-TC-6, alpha-TC-6, alpha-TC-3, and HepG2 cells were seeded in triplicate for each treatment group at ~400,000 cells/well in a 24-well tissue culture plate (#10062-896, VWR). Cells were incubated at 37°C and 5% CO_2 for 24 hours. The following day cells were treated with complete culture media containing 10 nM TCDD, DMSO vehicle control (#S276855, Sigma-

Aldrich), or no additives for 48 hours. Treatments were replenished after 24 hours.

Following 48-hour treatments, media was removed and cells were rinsed with PBS(-). Cells were released from the wells using a trypsin-EDTA (0.25%) solution (#25200072, Thermo Fisher Scientific) and quenched with culture medium. Each sample was collected into centrifuge tubes and centrifuged at 1200 rpm for 5 minutes. Total RNA was isolated using Qiagen RNeasy Mini kit (#74104, Qiagen) according to manufacturer protocol, with the exception of centrifuge times (30 seconds instead of 15 seconds). The quality and concentration of the RNA samples was measured using a NanoDrop (DeNovix DS-11 Spectrophotometer), wherein the A_{260}/A_{280} ratio was used to assess RNA purity. RNA samples were stored at -80°C.

Double stranded cDNA was synthesized using 250 ng of total RNA from each sample using the Bio-Rad iScript cDNA synthesis kit (#1708841, Bio-Rad) and a Bio-Rad T100 Thermocycler. DNA digestion (25°C for 5 minutes) and DNase inactivation (75°C for 5 minutes) were carried out using the iScript gDNA Clear kit (#1725035, Bio-Rad). Priming (25°C for 5 minutes), reverse transcription (42°C for 30 minutes), and inactivation (85°C for 5 minutes) were carried out using iScript Reverse Transcription Supermix (#1708841, Bio-Rad). cDNA samples were stored at -30°C.

Real time reverse transcription-quantitative PCR (RT-qPCR)

cDNA samples were diluted 1:10 in a 'master mix' consisting of forward and reverse primer mix, SsoAdvanced Universal SYBR Green Supermix (#1725274, Bio-Rad), UltraPure DNAse/RNAse-free dH_2O (#10977015, Invitrogen), and Precision Blue Real-Time PCR Dye (#1725555, Bio-Rad). Samples were loaded into a 384-well (#HSP3805, Bio-Rad) PCR plates. The RT-qPCR reaction was run according to the amplification protocol outlined in Table 1.1 on a Bio-Rad CFX384 Touch Real-Time PCR Detection System.

Table 1.1 RT-qPCR amplification protocol.

Step	Temperature (°C)	Time
1	95	1 minute
2	95	5 seconds
3	60	20 seconds
Return to Step 2 x 39 cycles		
5	65	5 seconds
6	95	50 seconds
7	4	∞

Changes in gene expression were calculated using the ΔΔCt method, using *HPRT* or *PPIA* housekeeping genes as an internal control. The genes (and their primer sequences) analyzed in this chapter are included in Table 1.2.

Table 1.2 Primer sequences used for gene expression analysis of rodent alpha and beta cell lines.

Gene	Species	Forward	Reverse
Cyp1a1	Human	GAACAAACAGGGCTGCCTTCT	GAGACCAATAGAAGGTAATTGAAATACCCC
Cyp1a1	Mouse	ATCACAGACAGCCTCATTGAGC	AGATAGCAGTTGTGACTGTGTC
Ahr	Mouse	AGCCGGTGCAGAAAACAGTAA	AGGCGGTCTAACTCTGTGTTC
Arnt	Mouse	GACAGACCACAGGACAGTTCC	AGCATGGACAGCATTTCTTGAA
PPIA	Human/ mouse	AGCTCTGAGCACTGGAGAGA	GCCAGGACCTGTATGCTTTA
Hprt	Mouse	GCTGACCTGCTGGATTACAT	TTGGGGCTGTACTGCTTAAC

Glucose-stimulated insulin secretion (GSIS)

INS-1 cells were chosen for GSIS as they secrete insulin in response to a high glucose environment. INS-1 cells were seeded at a density of 400,000 cells/well in a 24-well plate and incubated at 37°C and 5% CO_2 for 24 hours. Cells were then treated with 1 nM TCDD, 10 nM TCDD, or DMSO vehicle control for 48 hours. All treatments were replenished after 24 hours. On day 3, cells were ~95% confluent and ready for GSIS. Krebs-Ringer bicarbonate HEPES buffer (KRBH) solution (pH 7.4) (Table 1.3) was prepared the day of GSIS and filter sterilized. The appropriate volume of 2.5 M glucose (#G8769, Sigma-Aldrich) was added to each KRBH solution to achieve 2.8 mM and 16.7 mM final glucose concentrations.

The cells were rinsed with PBS(-) then incubated in 0 mM glucose KRBH for 1 hour at 37°C and 5% CO_2. The cells were then incubated in 2.8 mM (low) glucose KRBH for 1 hour at 37°C and 5% CO_2. The supernatant was collected and centrifuged at 13,000 rpm for 1 minute and 450 µL of the supernatant was

transferred to a new tube and stored at -20°C. Meanwhile, the cells were incubated in 16.7 mM (high) glucose KRBH for 1 hour at 37°C and 5% CO_2. After 1 hour the supernatant of the high glucose KRBH was collected as previously described and stored at -20°C. The cells were then incubated in acid-ethanol (1.5% HCl + 75% ethanol + ddH_2O) overnight at 4°C to collect total insulin content.

The next day, the insulin content from the acid-ethanol extraction was collected as previously described, then neutralized with 1 M Tris-base (pH 7.5) and stored at -20°C.

Table 1.3 KRBH solution components.

Component	Stock Concentration (M)	Final Concentration (mM)
NaCl	2	115
KCl	1	5
$NaHCO_3$	Added as powder	24
$CaCl_2$	1	2.5
$MgCl_2$	1	1
HEPES	1	10
BSA	Added as powder	0.1% w/v

GSIS Analysis: Enzyme-linked immunosorbent assay (ELISA)

Insulin content in each sample (low glucose, high glucose, and acid-ethanol) was quantified using high-range insulin ELISAs (#80-INSMSH-E10, Alpco). Absorbance was read on a Synergy H1 Multi-Mode microplate reader (BioTek Instruments).

Statistics

Statistical analyses were completed using GraphPad Prism 7 software. All data are presented as mean ± SEM with individual technical replicates shown. Specific statistical tests are indicated in the legend of each figure.

1.3 Results

Rodent alpha and beta cell lines were used to determine if TCDD is acting locally within either of the two most abundant endocrine cells in the pancreatic islets, thus inducing the production of Cyp1a1 enzymes. We hypothesized that the AhR pathway is present and inducible in the insulin-secreting beta cells. A high dose of 10 nM TCDD was chosen as it has previously been shown to maximally induce Cyp1a1 enzyme activity *in vitro* (Bofinger *et al*., 2001; Spencer *et al*., 1999) and to induce Cyp1a1 enzyme activity in mouse and human islets (Bruin lab, unpublished data). HepG2 cells were used as a positive control as they produce *CYP1A1* mRNA transcripts and enzyme activity in response to AhR agonists such as TCDD (Westerink and Schoonen, 2007).

A luminescence-based Cyp1a1 enzyme activity assay revealed that the HepG2 human liver cell line was appropriately responsive to TCDD exposure such that the luminescence associated with enzyme activity was ~22,000 RLU (Figure 1.1A). The enzyme activity of the rodent beta cell lines (MIN6, beta-TC-6, INS-1) was within the threshold of background-level luminescence; all were below 300 RLU (Figure 1.1A). Similarly, neither alpha cell line (alpha-TC-1, alpha-TC-3) produced functional Cyp1a1 enzymes, in contrast to the HepG2

positive control line, which again generated a luminescence of ~20,000 RLU following 48-hr TCDD exposure (Figure 1.1B)

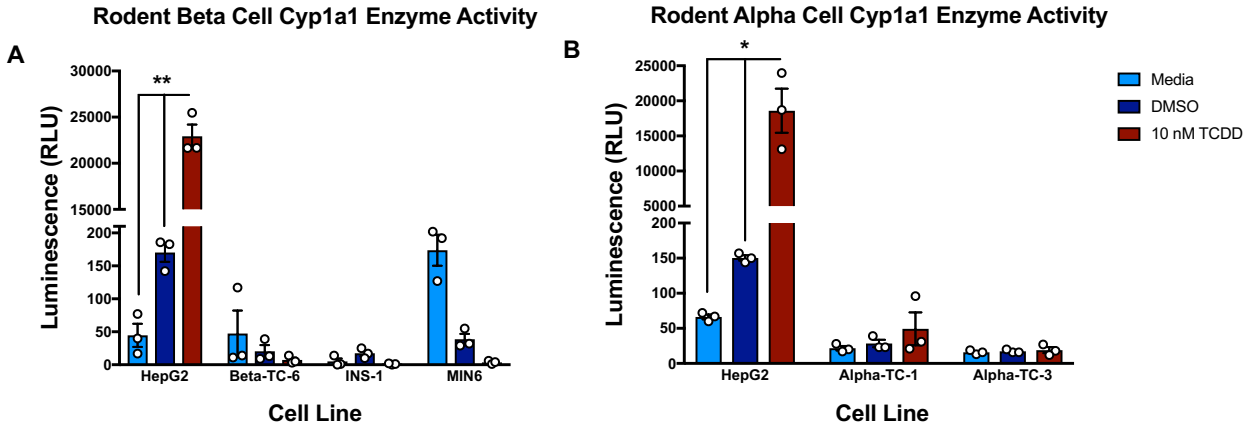

Figure 1.1 Cyp1a1 enzyme activity in rodent (A) beta and (B) alpha cell lines, and human liver control line following 10 nM TCDD treatment, DMSO vehicle control, or no additives (media) for 48 hours. **P<0.0001, *P<0.05 as determined by one-way ANOVA using Tukey's multiple comparisons test (N=3).

I next examined expression of *Cyp1a1, Ahr,* and *Arnt* genes in each cell line to determine if the rodent cells have the aryl hydrocarbon receptor complex (AhRC) machinery and if *Cyp1a1* gene expression might be increasing despite no enzyme activity. The rodent alpha and beta cell lines and human liver cell line were again treated with 10 nM TCDD, DMSO vehicle control, or no additives, and collected after 48 hours. As expected, RT-qPCR analysis revealed a pronounced ~300-fold increase in *CYP1A1* in the TCDD-exposed HepG2 cells (Figure 1.2). Interestingly, the INS-1 cells showed a modest but statistically significant ~3-fold increase in *Cyp1a1*, while the other beta and alpha cell lines did not show any increase in *Cyp1a1* following treatment with TCDD (Figure 1.2).

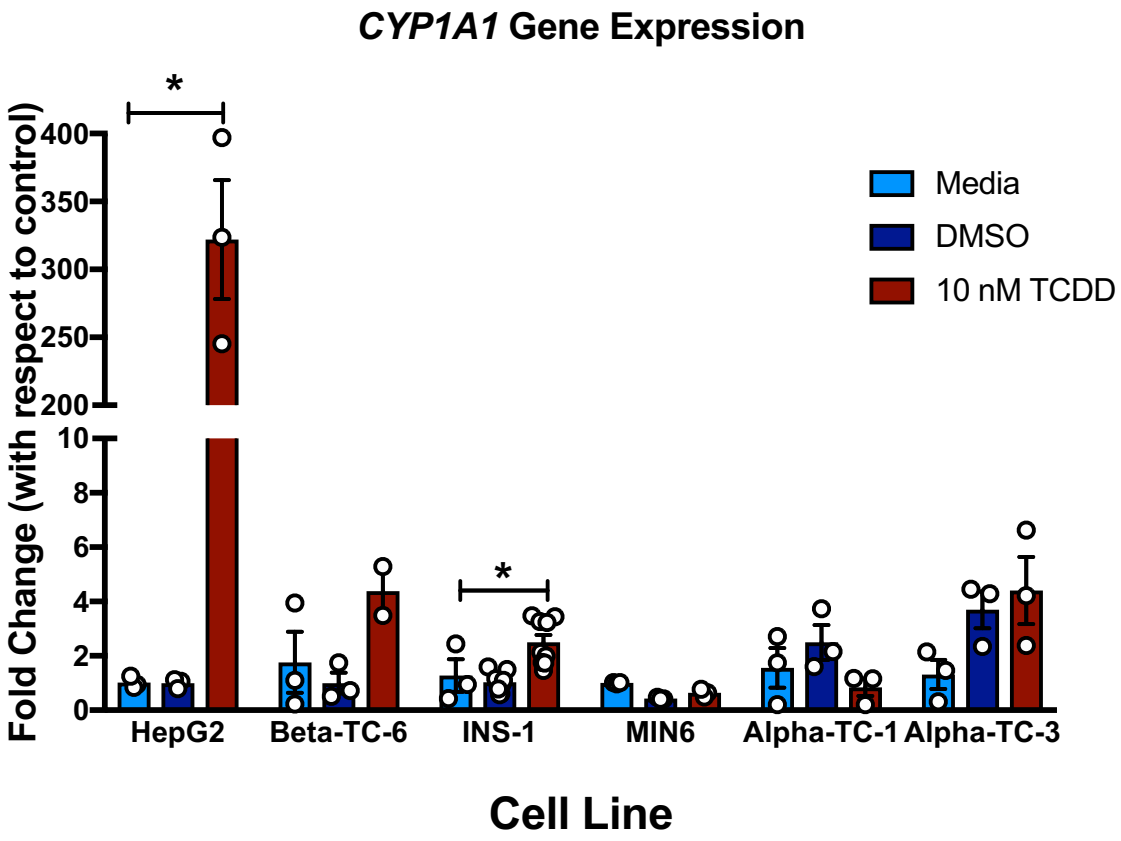

Figure 1.2 *Cyp1a1* gene expression in human liver control line, rodent beta cell lines, and rodent alpha cell lines following 48-hour exposure to 10 nM TCDD, DMSO vehicle control, or no additives (media). *P<0.05 as determined by one-way ANOVA using Tukey's multiple comparisons test (N=2-9).

Ahr and *Arnt* expression did not change in any of beta cell lines treated with TCDD (Figure 1.3, Figure 1.4), but were detectable in the MIN6, INS-1 and beta-TC-6 cells (Ct values ranging ~24-30). The alpha-TC-3 cells did not have detectable *Ahr* gene expression, while the alpha-TC-1 cells had consistently low *Ahr* gene expression (Ct values ~33) (Figure 1.3). *Arnt* was detectable and consistent in both alpha-TC-1 and alpha-TC-3 lines but did not change in cells exposed to TCDD compared to those exposed to the DMSO vehicle control (Ct

values ~24) (Figure 1.4). Functional human *AhR* and *ARNT* primers have not yet been identified; therefore these genes have not yet been evaluated in the HepG2 liver line.

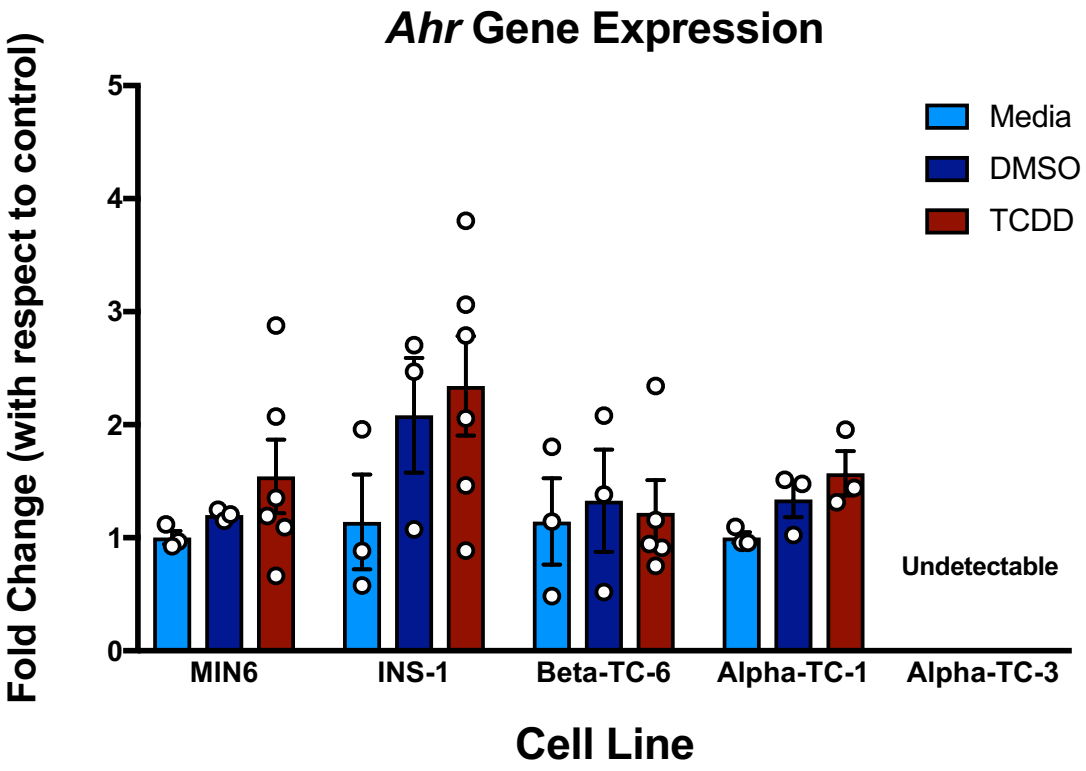

Figure 1.3 *Ahr* gene expression in rodent beta and alpha cell lines following 48-hour exposure to TCDD, DMSO vehicle control, or no additives (media). No statistical significance as determined by one-way ANOVA using Tukey's multiple comparisons test (N=3-6).

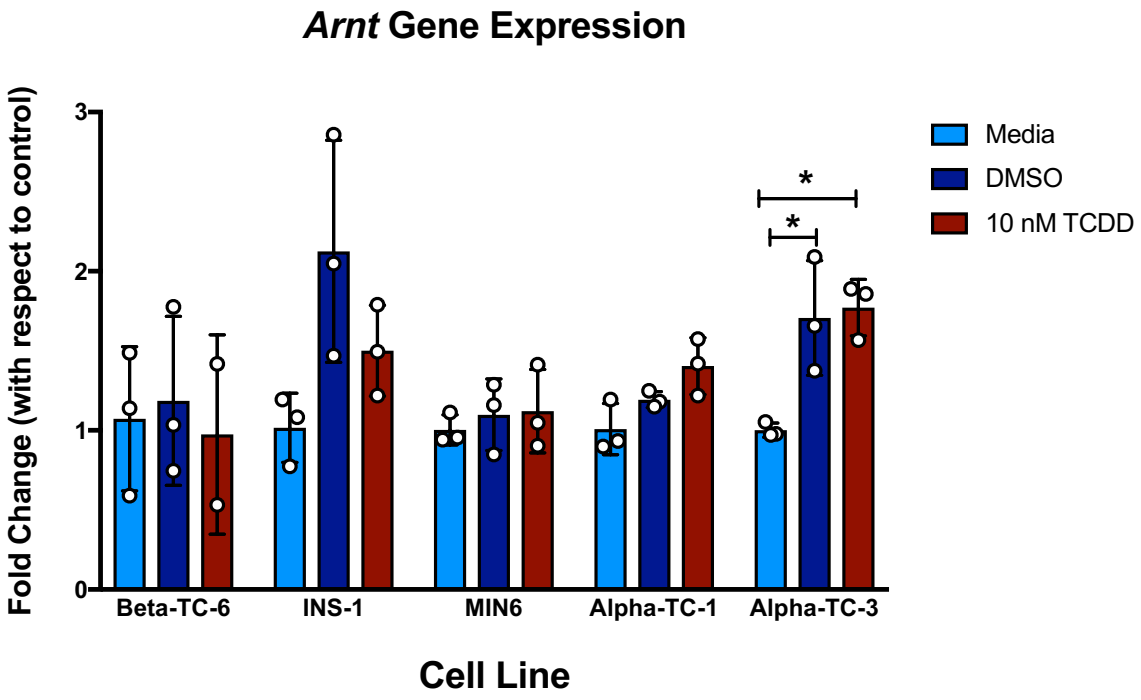

Figure 1.4 *Arnt* gene expression in rodent beta and alpha cell lines following 48-hour exposure to TCDD, DMSO vehicle control, or no additives (media). *P<0.05 as determined by one-way ANOVA using Tukey's multiple comparisons test (N=3-6).

Finally, I performed a glucose-stimulated insulin secretion (GSIS) test on the INS-1 beta cells treated with 1 nM, 10 nM TCDD, or DMSO vehicle control for 48 hours to assess changes in insulin secretion. Insulin ELISA analysis revealed no change in insulin secretion in the INS-1 cells treated with 1 nM or 10 nM TCDD compared to control (Figure 1.5). Total insulin content of each sample was determined following overnight extraction by acid-ethanol. The 1 nM and 10 nM TCDD-treated cells appear to have slightly higher insulin content than the DMSO-treated control cells, despite all samples having the same confluence (all nearly

100%; Figure 1.5). There was no statistical significance but the TCDD-treated cells are trending toward higher basal insulin content.

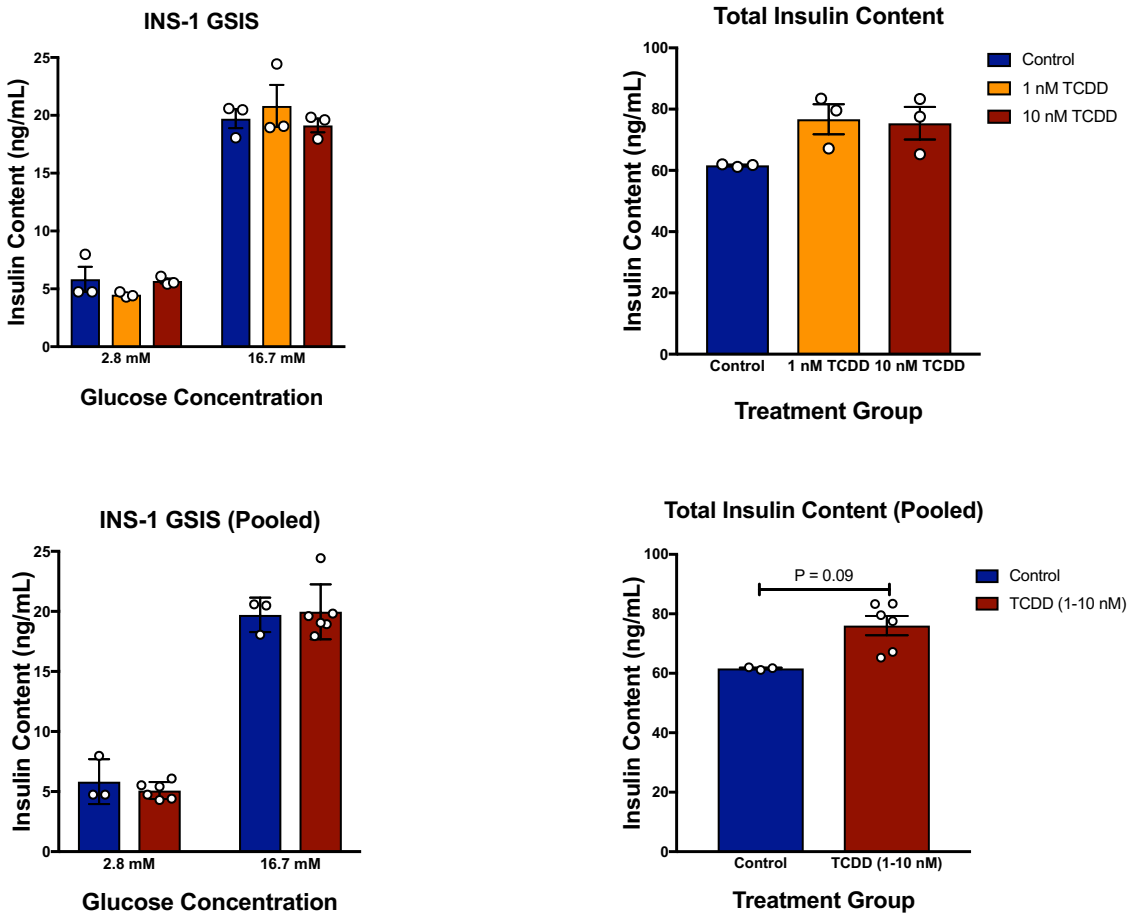

Figure 1.5 Glucose-stimulated insulin secretion in INS-1 cells following 48-hour treatment with DMSO vehicle control, 1 nM TCDD, or 10 nM TCDD (no significance, one-way ANOVA, N=3) and total insulin content released by acid-ethanol extraction (no significance, one-way ANOVA, N=3). Pooled data (1 nM and 10 nM combined) is shown below (P=0.09 as determine by unpaired t-test).

1.4 Discussion

The primary goal of this chapter was to use rodent alpha and beta cell lines to determine which in which pancreatic cell type TCDD induces production of Cyp1a1 enzymes as seen *in vivo*. To address this question, I implemented three rodent beta cell lines, two rodent alpha cell lines, and one human liver cell line to study Cyp1a1 enzyme activity and gene expression *in vitro*. A luminescence-based activity assay revealed no functional Cyp1a1 enzymes in any of the rodent alpha or beta cell lines, unlike the positive control human liver cell line following a 48-hour exposure to 10 nM TCDD. This means that TCDD is not inducing Cyp1a1 enzyme production in the rodent cell lines.

Further investigation of *Cyp1a1* gene expression showed no increase in *Cyp1a1* in the alpha cell lines, MIN6, or beta-TC-6 lines following treatment with TCDD, though a modest increase was noted in the INS-1 cells. The ~3-fold increase seen in the INS-1 cells is subtle and considering the lack of enzyme activity, it can be concluded that the INS-1 cells are not a suitable model of human beta cell physiology in this context and cannot be used to explain the significant Cyp1a1 enzyme activity and gene expression found in both mouse and human islets treated with TCDD. It is also important to consider that beta cells alone function differently than those within intact islets. Islets contain numerous endocrine cell types that provide paracrine cues essential for normal function. Therefore, while immortalized rodent cell lines would be a convenient model system of beta cell physiology, they are inherently different than true human beta cells.

Together, alpha and beta cells comprise ~90% of human pancreatic islets, therefore it makes sense that if islets are producing Cyp1a1 enzymes after exposure to TCDD that one of these two endocrine cells could be producing these enzymes. One study showed that *Cyp1a1* is an ethanol-inducible gene in hamster insulinoma (HIT) cells, which tells us that the machinery responsible for *Cyp1a1* transcription is at least present in insulin-producing cells (Shin *et al*., 2004). To determine if the genes involved in the AhR pathway are present in any of the rodent cell lines, I explored *Ahr* and *Arnt* expression following treatment of 10 nM TCDD for 48 hours. I found that both *Ahr* and *Arnt* are detectible in the three rodent beta cell lines, but their expression does not change with exposure to TCDD. Interestingly, the alpha-TC-3 line did not have detectable *Ahr* while the alpha-TC-1 line had detectable but low expression. *Arnt* was detectable and consistent in both alpha cell lines. This finding might suggest that the AhR pathway is not functional in the alpha-TC-3 cells.

In humans, ARNT is not only involved in translocation of the AhR-ligand complex to the nucleus, but is also a co-factor for transcriptional regulation by hypoxia-inducible factor (HIF) 1 and is also known as HIF-1β. Its role is key for cellular adaptations to environmental stressors including hypoxia and dioxins/dioxin-like compounds (Mandl and Depping, 2014). This might explain why *Arnt* expression is detectable even if *Ahr* expression is low or undetectable. Further, a protein called aryl hydrocarbon receptor repressor (AhRR) has been identified in both human and rat genomes (Vogel and Haarmann-Stemmann, 2017). Transcription of AhRR is activated once xenobiotic response elements are

bound following activation of AhR by a ligand (Noakes, 2015). AhRR is capable of inhibiting AhR, possibly by competing for co-activating molecules involved in the AhR pathway (Vogel and Haarmann-Stemmann, 2017). This effectively produces a negative-feedback pathway for AhR activity, which might explain why after 48 hours of TCDD exposure there isn't a marked increase in *Ahr* compared to controls. Pollenz (1996) showed that AhR protein in Hepa-1c1c7 (murine hepatoma) cells exposed to TCDD was decreased by 85% after just 4 hours of exposure, while Arnt expression was unaffected. Non-hepatic cell types demonstrated this same trend of AhR depletion following TCDD exposure (Pollenz, 1996).

Unfortunately, I have yet to identify primers that recognize human *AhR* and *ARNT*, which could be used to study changes in gene expression in HepG2 human cells exposed to TCDD. Once I design and validate new primers for these targets, I will be able to compare the rodent beta cell data to HepG2, where the AhR pathway is functional as determined by *CYP1A1* gene expression and enzyme activity assay.

Glucose-stimulated insulin secretion is an effective method for evaluating changes in pancreatic beta cell physiology. When introduced to a hyperglycemic environment, beta cells are triggered to secrete insulin in order to reduce the circulating glucose levels (e.g. by promoting glucose uptake and storage into tissues *in vivo*). When treated with either 1 nM or 10 nM TCDD for 48 hours the INS-1 cells showed no change in their ability to secrete insulin in response to a high glucose stimulus compared to control. However, total insulin content trended

towards being higher in TCDD-treated cells (1 nM or 10 nM). Interestingly, one study showed that INS-1 cells treated with low doses (0.05-1 nM) of TCDD for just one hour resulted in impaired GSIS (Piaggi *et al*., 2007). Another group demonstrated an increase in insulin secretion in INS-1 cells following exposure to higher doses of TCDD (10-100 nM) and suggested TCDD may induce continuous insulin release via increased cytosolic calcium content, which could eventually lead to beta cell exhaustion (Kim *et al*., 2009). In the context of the data presented here, it is possible that the INS-1 cells are mirroring the effects seen by Kim *et al.* (2009), however it is more likely that the cells are unaffected by a 48-hour exposure to TCDD considering the lack of *Cyp1a1* gene expression and enzyme activity, which indicates the AhR pathway is not active in these cells.

The second goal of this study was to evaluate rodent endocrine cell lines as a model for studying the impact of other dioxin-like pollutants *in vitro*. While rodent cell lines are widely accessible and easy to maintain in culture, they do not behave as true alpha and beta cells. This limits their use for *in vitro* studies of human endocrine cell physiology. I discovered here that none of the rodent cell lines tested (MIN6, beta-TC-6, INS-1, alpha-TC-1, and alpha-TC-3) were able to produce active Cyp1a1 enzymes following exposure to TCDD, the most potent ligand for AhR. I can therefore conclude that these lines are not appropriate for screening other dioxin-like chemicals for Cyp1a1 enzyme activity and physiological changes in alpha or beta cells.

1.5 Conclusions and Future Directions

To complete this story, I will analyze gene expression of *AhR* and *ARNT* in human HepG2 cells, as well as *Ins*, *Mafa*, *Gcg,* and *Mafb* in the rodent cell lines. The human liver cell line will provide insight into whether TCDD is decreasing the expression of *AhR* in a negative-feedback loop, hence why expression was low or undetectable in the rodent cells, or if the rodent cells generally lack the AhR machinery required to respond to TCDD. The alpha and beta cell-specific genes will provide more information about the physiological identities of the rodent endocrine cells.

In conclusion, rodent endocrine cells are insufficient models of pancreatic islet cell physiology for studying the response to dioxin and dioxin-like chemicals. I therefore implemented human embryonic stem cells as a model of human development to further investigate the impact TCDD might have on the developing pancreas.

Chapter 2: Optimization of human embryonic stem cell differentiation

2.1 Introduction to human embryonic stem cells

Human embryonic stem cells (hESCs) are a versatile model system for studying human development. hESCs are derived from the inner cell mass of a blastocyst and eventually form the tissues of the fetus *in utero*. The outer layer of the blastocyst is called the trophoblast, which becomes the placenta for the fetus. hESCs are considered pluripotent because they have the potential, if given the right environmental cues, to develop into any cell in the human body. In a laboratory setting we can control the development of stem cells into specific cell types; this is known as differentiation. Embryonic stem cells are also highly proliferative and can therefore be cultured *in vitro*.

Protocols have been established for hESC differentiation into various lineages that mimic developmental programs. Of interest to our lab is human pancreas development. I attempted to implement a 7-stage differentiation protocol described in Rezania *et al*., 2014, that generates 'maturing beta cells'. The 7 stages of *in vitro* pancreatic development are: 'Stage 1: definitive endoderm', 'Stage 2: primitive gut tube', 'Stage 3: posterior foregut', 'Stage 4: pancreatic endoderm', 'Stage 5: pancreatic endocrine precursors', 'Stage 6: immature beta cells, and 'Stage 7: maturing beta cells' (Figure 2.1).

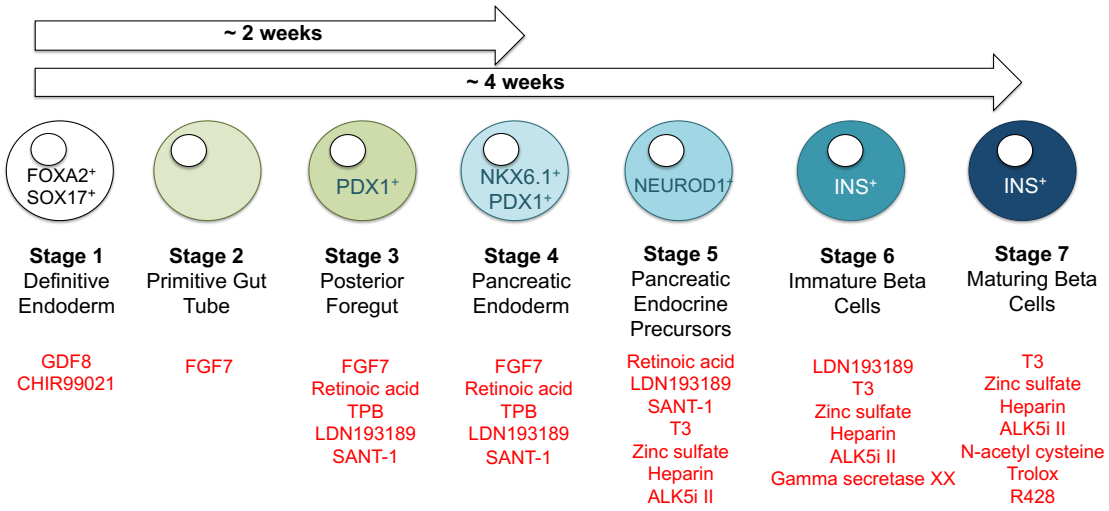

Figure 2.1 Summary of human pancreatic beta cell development and corresponding stages of hESC differentiation. Stage-specific additives are indicated in red.

My primary goal was to initiate and optimize the differentiation protocol described in Rezania *et al*., 2014. In this chapter I discuss some of the troubleshooting experiments I performed and my progress thus far.

2.2 Methods

Human embryonic stem cell culture maintenance

In order to start culturing cells, I had to first establish an inventory of reagents, consumables, and tools required of a tissue culture facility. Differentiation reagents and additives were also prepared into working stocks and stored at -80°C (Table 2.1).

Table 2.1 Differentiation additives stock details.

Additive	[Stock]	Final Dilution	Details
GDF8	100 µg/mL	1000X	#120-00, PeproTech
Activin A	100 µg/mL	1000X	#338-AC, R&D
CHIR99021	4015 µM	4015X	#SML1046, Sigma-Aldrich
FGF7	50 µg/mL	1000X	#100-19, Peprotech
Retinoic acid	1 mM	1000X	#R2625, Sigma-Aldrich
TPB	200 µM	1000X	#565740, Sigma-Aldrich
LDN193189	100 µM	1000X	#SML0559, Sigma-Aldrich
SANT-1	0.25 mM	1000X	#J65294-MA, Alfa Aesar

Human embryonic stem cells (WA01 or H1) were purchased from WiCell Institute (Madison, WI) and cultured several passages prior to establishing a large cell bank. To do this, Matrigel (#CACB356231, VWR) was diluted 1:30 in DMEM/F12 media (#11-330-032, Fisher Scientific) and used to coat two wells of a 6-well plate (#140675, Thermo Fisher Scientific). H1 cells were initially thawed into two wells in 'Essential 8' medium (produced by the Ottawa-Hospital Research Institute Human Pluripotent Stem Cell Facility), plus 10 µM Y-27632 (#1254, Tocris) for one day only. Cells were incubated at 37°C and 5% CO_2 and media changes were performed daily. Colonies were monitored daily via light microscopy for regions of spontaneous differentiation, indicated by changes in morphology and colony overgrowth. Differentiated cells were removed using a pipette tip under a microscope (Zeiss) in a laminar flow hood.

When ready to passage (~80% confluent), cells were rinsed with PBS(-) and then incubated in 1X Versene (#15040-066, Gibco) for 3-5 minutes at 37°C and 5% CO_2. Versene was removed and fresh media was added. Cells were collected with a cell scraper (#83.1832, Sarstedt) and colonies were broken up gently by pipetting then distributed to new Matrigel-coated plate(s). Once

expanded into several 6-well plates, an initial bank of H1 cells was created. Cells were frozen with mFreSR (#05855, STEMCELL Technologies) and stored in the vapour phase of liquid nitrogen. Cells were also tested for mycoplasma as previously described.

The H1 cells were eventually transitioned to mTeSR1 (#85850, STEMCELL Technologies) and an improvement in culture quality was observed (less spontaneous differentiation and more consistent passage time). At this point, the H1 cells were also scaled up in T-75 tissue culture flasks (#13-680-65, Fisher Scientific) and the cell bank was expanded again. Currently, H1 cells are cultured in mTeSR Plus medium (#05825, STEMCELL Technologies), which allows for more time between media changes.

Single-cell seeding for differentiation

H1 cells were cultured as described in T75 tissue culture flasks. Following at least two passages post-thaw, cultures were rinsed with PBS(-), then incubated in TrypLE Express (#12604-021, Thermo Fisher Scientific) for up to 6 minutes at 37°C and 5% CO_2. The dissociation reaction was quenched with fresh mTeSR1 medium and centrifuged at 1200 rpm for 5 minutes. The pellet was thoroughly resuspended in fresh mTeSR1 with 10 µM Y-27632, counted using a Countess II Automated Cell Counter (Thermo Fisher Scientific), and plated at 250,000 cells/well in 1:30 Matrigel-coated 24-well plates (#10062-896, VWR). Cells were incubated at 37°C and 5% CO_2 for 24 hours. The following day fresh

media without Y-27632 was added to the wells. Differentiation was initiated 48 hours after seeding. Cells were ~80% confluent prior to starting differentiation.

Flow cytometry analysis

Cells to be collected for flow cytometry analysis were rinsed with PBS(-), then incubated in TrypLE Express for 2 minutes at 37°C and 5% CO_2. The dissociation reaction was quenched with basal media, and cells were centrifuged at 1200 rpm for 5 minutes.

Intracellular Targets

Cells were resuspended in 250 µL/sample of Fixation and Permeabilization solution (#554722, BD) and fixed at 4°C for 1 hour. Cells were then centrifuged at 1800 rpm for 1 minute, and then washed twice in 250 µL Perm/Wash buffer (#554723, BD). Cells were stained with appropriate intracellular antibody (or co-stained with two antibodies) diluted with Perm/Wash buffer according to Table 2.2 for 1 hour at 4°C in the dark. Cells were centrifuged at 1800 rpm for 1 minute then washed twice in 250 µL Perm/Wash buffer. Each sample was resuspended in 200 µL PBS + 5% FBS (#F51051, Sigma-Aldrich) ('PBS/FBS') and analyzed on a BD Biosciences Accuri C6 flow cytometer.

Cell Surface Markers

Cells were washed twice in 250 µL PBS/FBS then stained with appropriate cell surface antibody diluted in PBS/FBS for 1 hour at 4°C in the dark. Cells were then centrifuged at 1800 rpm for 1 minute and washed twice with 250 µL

PBS/FBS. Each sample was resuspended in 200 µL PBS/FBS and analyzed on a BD Biosciences Accuri C6 flow cytometer.

Antibody Optimization

Each antibody used for stage-specific markers of differentiation was validated and dilutions were optimized with respect to positive and negative cells. For example, to validate and optimize PDX1, the positive cells were a rodent beta cell line and the negative cells were pluripotent hESCs (H1 cells). The optimal antibody dilutions are shown in Table 2.2. All antibodies are conjugated.

Table 2.2 Antibodies used for flow cytometry analysis of stage-specific markers of differentiation.

Antibody	Fluorophore	Dilution	Type	Details
OCT4	PE	1:100	Intracellular	#560186 (BD)
SOX2	PE	1:100	Intracellular	#IC2018P (R&D)
CXCR4	PE	1:10	Cell surface	#555974 (BD)
SOX17	PE	1:100	Intracellular	#561591 (BD)
FOXA2	Alexa Fluor 488	1:100	Intracellular	#IC2400G (R&D)
PDX1	PE	1:20	Intracellular	#562161 (BD)
NKX6.1	PE	1:20	Intracellular	#563023 (BD)
IgG1, k	PE			#555749 (BD)
IgG2a, k	PE			#555574 (BD)

Stem cell differentiation protocol

The Rezania *et al*., 2014 protocol is a 28-day differentiation program that generates glucose-responsive insulin-secreting beta-like cells. H1 cells were seeded according to single-cell seeding protocol described above. Basal media formulations were organized into four distinct categories (A-D), and pre-prepared at the start of each stage (Table 2.3). Stage-specific additives were introduced to

the required volume of basal media each day (Table 2.4). Media was changed at the same time (± 1 hour) each day. At the end of each stage a subset of cells was collected for flow cytometry and PCR (described in **Chapter 1**) analysis of stage-specific markers of differentiation, and images of the cells were taken on an EVOS FL microscope.

Table 2.3 Basal media formulations throughout differentiation.

Stage	Media	Components	Details
1	A	MCDB 131 medium Glutamax (1X) Glucose (10 mM) BSA (0.5%) Sodium bicarbonate (1.5 g/L)	#15-100-CV (Corning) #35050061 (Fisher) #G8769 (Sigma) #10775835001 (Sigma) #S233-500 (Fisher)
2	B	MCDB 131 medium Glutamax (1X) Glucose (10 mM) BSA (0.5%) Sodium bicarbonate (1.5 g/L) Ascorbic acid (0.25 mM)	 #A4544 (Sigma)
3	C	MCDB 131 medium Glutamax (1X) Glucose (10 mM) BSA (2%) Sodium bicarbonate (2.5 g/L) Ascorbic acid (0.25 mM) ITS-X (1:200)	 #51500-056 (Fisher)
4	C	Same as above	Same as above
5	D	MCDB 131 medium Glutamax (1X) Glucose (20 mM) BSA (2%) Sodium bicarbonate (1.5 g/L) ITS-X (1:200)	Same as above
6	D	Same as above	Same as above
7	D	Same as above	Same as above

Table 2.4 Differentiation timeline and required additives, adapted from Rezania *et al*., 2014 (see Table 2.1 for additive information),

Stage	Day	Basal Media	Additives
1	1	A	Activin A or GDF8 (100 ng/mL) CHIR99021 (1 μM)
	2	A	Activin A or GDF8 (100 ng/mL) CHIR99021 (0.1 μM)
	3	A	Activin A or GDF8(100 ng/mL)
2	4	B	FGF7 (50 ng/mL)
	5	B	Same as Day 5.
3	6	C	FGF7 (50 ng/mL) Retinoic acid (1μM) TPB (200 nM) LDN193189 (100 nM) SANT-1 (0.25 μM)
	7	C	Same as Day 6.
4	8	D	FGF7 (2 ng/mL) Retinoic acid (0.1 μM) TPB (100 nM) LDN193189 (200 nM) SANT-1 (0.25 μM)
	9	D	Same as Day 8.
	10	D	Same as Day 8.
5	11	D	Retinoic acid (0.05 μM) LDN193189 (100 nM) SANT-1 (0.25 μM) T3 (1 μM) Zinc sulfate (10 μM) Heparin (10 μg/mL) ALK5i II (10 μM)
	12	D	Same as Day 11.
	13	D	Same as Day 11.
6	14	D	LDN193189 (100 nM) T3 (1 μM) Zinc sulfate (10 μM) Heparin (10 μg/mL) ALK5i II (10 μM) Gamma secretase XX (100 nM)
	15	D	Same as Day 14.
	16	D	Same as Day 14.
	17	D	Same as Day 14.
	18	D	Same as Day 14.
	19	D	Same as Day 14.
	20		Same as Day 14.
7	21	D	T3 (1 μM) Zinc sulfate (10 μM)

			Heparin (10 µg/mL) ALK5i II (10 µM) N-acetyl cysteine (1 mM) Trolox (10 µM) R428 (2 µM)
	22	D	Same as Day 21.
	23	D	Same as Day 21.
	24	D	Same as Day 21.
	25	D	Same as Day 21.
	26	D	Same as Day 21.
	27	D	Same as Day 21.
	28	D	Same as Day 21.

Stage 1 Optimization: Seeding density and CHIR99021

To determine optimal starting conditions for differentiation including seeding density and CHIR99021 concentration, H1 cells were seeded at densities of 200,000-300,000 cell/well in 1:30 Matrigel-coated 24-well tissue culture plates. Cells were seeded according to above protocol.

Stage 1 Day 1 of the differentiation was initiated 48 hours post-seeding. H1 cells were treated in duplicate with basal Media A (Table 2.2) further supplemented with 100 ng/mL GDF8 and 0.5 µM, 1 µM, 1.5 µM, or 2 µM CHIR99021. On Stage 1 Day 2 the cells were exposed to basal Media A further supplemented with 100 ng/mL GDF8 and 0.1 µM CHIR99021. On Stage 1 Day 3 the cells were exposed to basal Media A further supplemented with 100 ng/mL GDF8 only. Cellular morphology and cell death were evaluated daily using an EVOS FL microscope.

On day 4 of differentiation, cells were collected for flow cytometry analysis of key Stage 1 markers of development, CXCR4, SOX17, and FOXA2.

Stage 1 Optimization: Activin A versus GDF8

GDF8 and Activin A are both members of the transforming growth factor beta (TGF-β) family of proteins, and when combined with a GSK3 inhibitor such as CHIR99021, induce the Nodal/Wnt signalling pathway, which directs hESCs toward definitive endoderm (Naujok *et al*., 2014; Rostovskaya *et al*., 2015; Wang *et al*., 2015). GDF8 is used in Rezania *et al*., 2014, but many other groups have published highly efficient DE protocols using Activin A (Wang *et al*., 2015; Pagliuca *et al*., 2014). We wanted to compare differentiation efficiency at Stage 1 for two combinations of Stage 1 additives, GDF8 + CHIR99021 versus Activin A + CHIR99021. This experiment was done in collaboration with our lab technician, Kayleigh Rick.

H1 cells were seeded as described above, into 12 wells of a 24-well plate. Cells were treated in duplicate according to the conditions outlined in Table 2.5. Images were taken of the cells every day of the differentiation on an EVOS FL microscope. At the end of Stage 1 cells were collected for flow cytometry analysis as described above. Cells were stained for CXCR4 and SOX17/FOXA2. A total of 10,000 cells from each sample were analyzed (BD Accuri C6).

Table 2.5 Differentiation conditions and timeline for Stage 1 (GDF8 vs Activin A)

	Day 1			**Day 2**			**Day 3**		
Condition	GDF8 (ng/ml)	Activin A (ng/ml)	CHIR (μM)	GDF8 (ng/ml)	Activin A (ng/ml)	CHIR (μM)	GDF8 (ng/ml)	Activin A (ng/ml)	CHIR (μM)
1	100		1	100		0.1	100		
2		100	0.5		100	0.05		100	
3		100	1		100	0.1		100	
4		100	1.5		100	0.15		100	
5		100	2		100	0.2		100	
6		100	3		100	0.3		100	

Optimization to Stage 4: Activin A versus GDF8

H1 cells were seeded as described above into a 24-well plate. Cells were differentiated using the Rezania *et al*., 2014 protocol, using either GDF8 or Activin A during Stage 1. During Stages 2-4 each well was treated the same with no further changes to the protocol. At each stage, cells were collected for flow cytometry analysis using antibodies indicated in Table 2.2, as previously described.

2.3 Results and Discussion

Example of a moderately successful differentiation

Prior to much of the troubleshooting I conducted, I was getting inconsistent differentiation efficiency. Figure 2.2 is an example of a moderately successful differentiation up to Stage ('S') 4 (pancreatic endoderm). *OCT4* is a marker of pluripotency and is highest in hESCs (S0). *OCT4* gradually starts to decrease in S1 through S4 (Figure 2.2 inset). Gene expression analysis of key markers of development shows increases in expression of two S1 (definitive endoderm) markers, *CXCR4* and *SOX17*, transiently during S1. These markers start to decrease in S2 and are non-detectable in S3. Expression of S3 (posterior foregut) marker, *PDX1*, is markedly increased in S3, but inappropriately decreased in S4. Essentially no *NKX6.1* gene expression was present in S4 (Figure 2.2). These data indicate that the differentiation progressed until S3 but failed at the transition to S4. mRNA from H1 ('S0') cells (N=2) and human islets (N=1) were used to compare changes in gene expression as the cells progressed toward the pancreatic lineage.

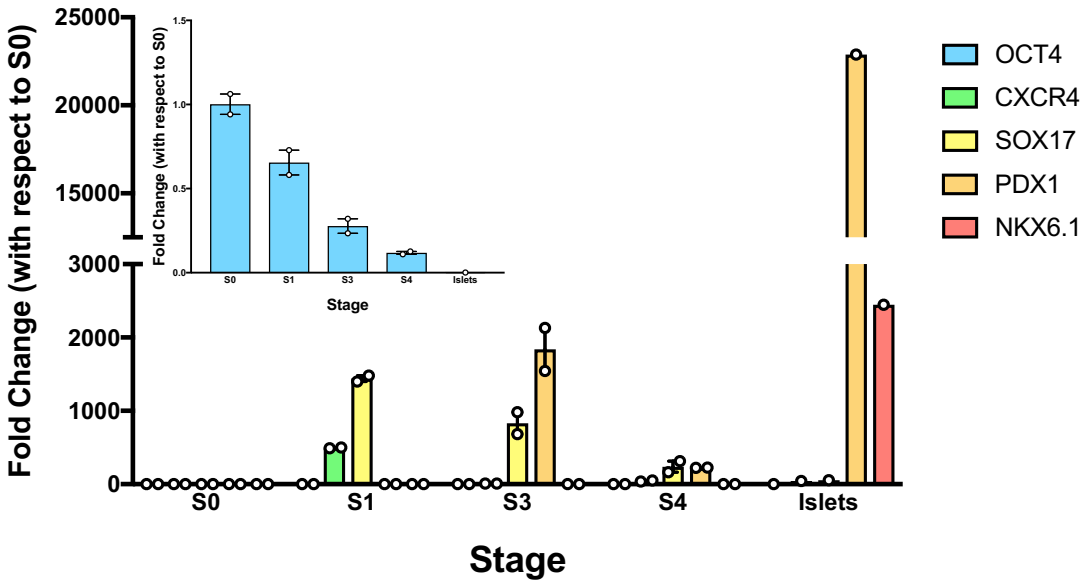

Figure 2.2 Gene expression of key markers of pancreatic development at different stages of differentiation toward Stage 4 'pancreatic endoderm'. *OCT4* expression is displayed in graph inset.

Stage 1 Optimization: Seeding density and CHIR99021

At the end of Stage 1, cells were collected for flow cytometry analysis of three key definitive endoderm markers (CXCR4, SOX17, and FOXA2). The combination of seeding density and Stage 1 Day 1 (S1D1) CHIR99021 concentration that produced the most efficient definitive endoderm populations was 250,000 cells/well and 1 μM CHIR99021. This combination resulted in ~95% CXCR4+ cells and ~91% of cells co-expressing SOX17 and FOXA2 (Figure 2.3). Going forward, seeding at a density of 250,000 cells and with 1 μM CHIR99021 on S1D1 should produce efficient Stage 1 definitive endoderm cells.

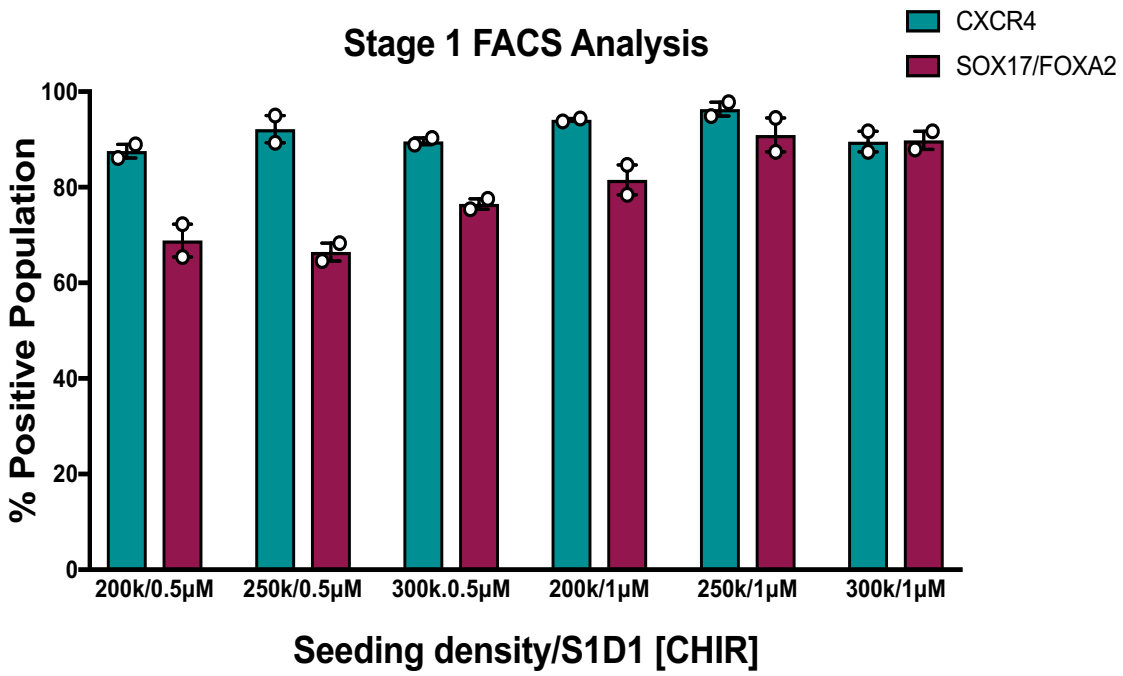

Figure 2.3 FACS analysis of H1 cells seeded at various densities treated with different Stage 1 Day 1 (S1D1) concentrations of CHIR99021. GDF8 was kept at 100 ng/mL during Stage 1. Live cells were stained with a CXCR4 antibody while fixed cells were co-stained with SOX17 and FOXA2 antibodies.

Stage 1 Optimization: Activin A versus GDF8

At the end of S1, cells were collected for flow cytometry analysis of three key definitive endoderm markers (CXCR4, SOX17, and FOXA2). Important to note, the cells treated with Activin A + 3 µM CHIR99021 had cell death at the centre of the wells, and one of the wells yielded a small pellet and small flow cytometry sample upon collection. Samples with little to no cells during flow cytometry analysis were omitted. Flow cytometry analysis revealed that GDF8 + 1 µM CHIR99021 and Activin A + 2 µM CHIR99021 yielded the most efficient Stage 1 ‘definitive endoderm’ cells (Figure 2.4). The GDF8/1 µM CHIR99021 combination resulted in ~86% CXCR4 and SOX17/FOXA2 efficiencies, while Activin A/2 µM CHIR99021 resulted in ~73% CXCR4 and ~82% SOX17/FOXA2

efficiencies (Figure 2.4). I later compared downstream efficiency of cells treated with GDF8 versus Activin A in S1.

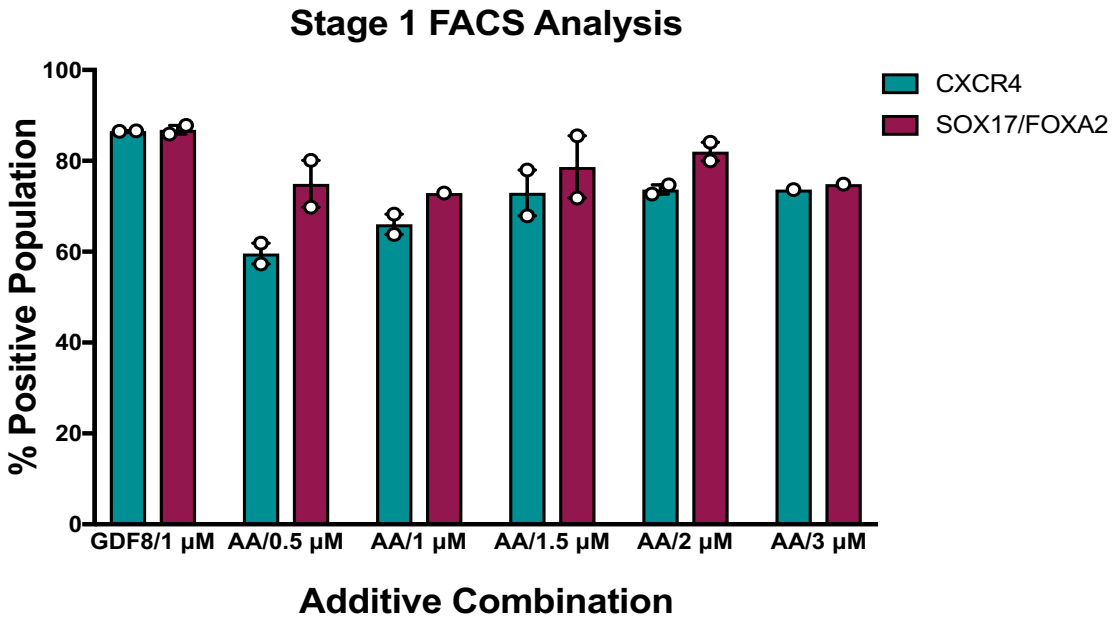

Figure 2.4 FACS analysis of H1 cells treated with various combinations of Stage 1 additives. GDF8 and Activin A (AA) were kept at 100 ng/mL during Stage 1 while CHIR99021 was titrated. Live cells were stained with a CXCR4 antibody while fixed cells were co-stained with SOX17 and FOXA2 antibodies.

Images of the differentiating cells were taken each day. Figure 2.5 shows cells on collection day (i.e. Day 4 of differentiation; S1D4). GDF8 and Activin A/1.5 µM CHIR99021 have the most homogenous populations viewed at 10X and 20X magnification (Figure 2.5). Other concentrations of CHIR99021 lead to 'plaque-like' regions in the differentiating populations and multiple areas of overgrowth of cells.

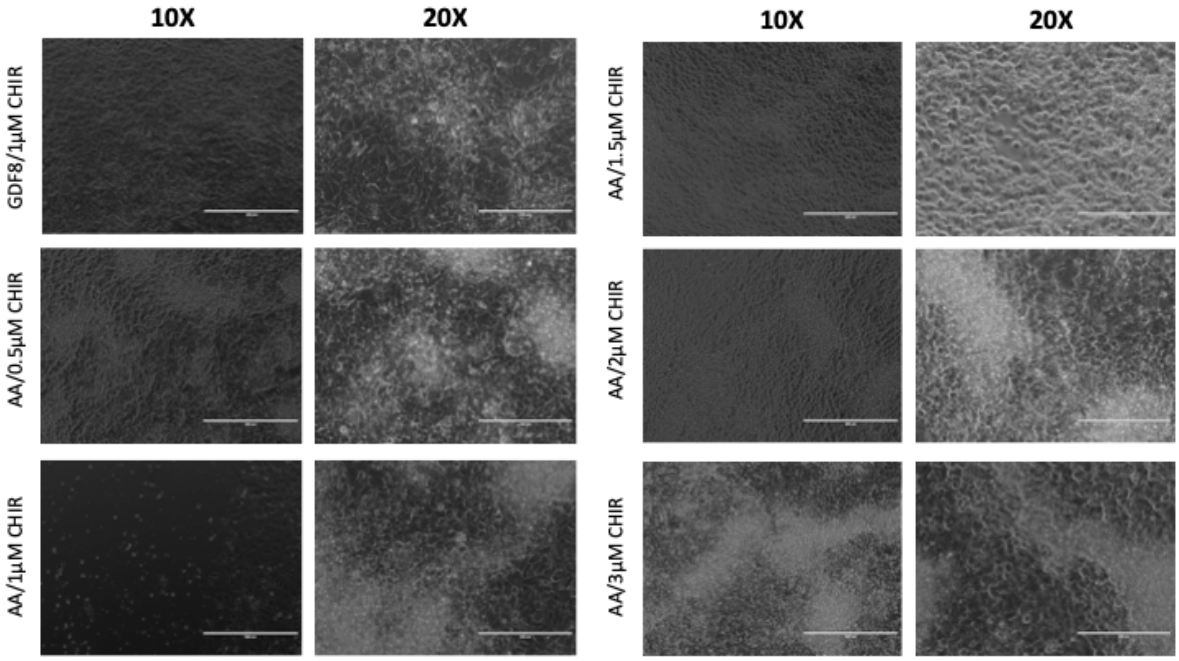

Figure 2.5 Stage 1 (definitive endoderm) cells differentiated with either GDF8 or Activin A and increasing concentrations of CHIR99021. Images taken with EVOS FL light microscope. Scale bars represent 400 μm (10X) and 200 μm (20X).

I also performed a second experiment where cells were treated with either GDF8 (100 ng/mL) or Activin A (100 ng/mL) in S1 and then continued through until S4. Cells were collected at the end of each stage and the efficiency of each differentiation (GDF8 versus Activin A treated) was assessed using flow cytometry. At S1, the Activin A treated cells had approximately 90% SOX17/FOXA2 co-positive cells, while the GDF8 treated cells had around 75% co-positive cells (Figure 2.6).

Analysis of S2 populations again revealed ~90% SOX17+/FOXA2+ cells in those treated with Activin A in S1 compared to ~75% SOX17+/FOXA2+ in cells

treated with GDF8 in S1. The Activin A treated cells also had ~80% OCT4+/FOXA2+ cells compared to ~65% in the GDF8-treated cells (Figure 2.7)

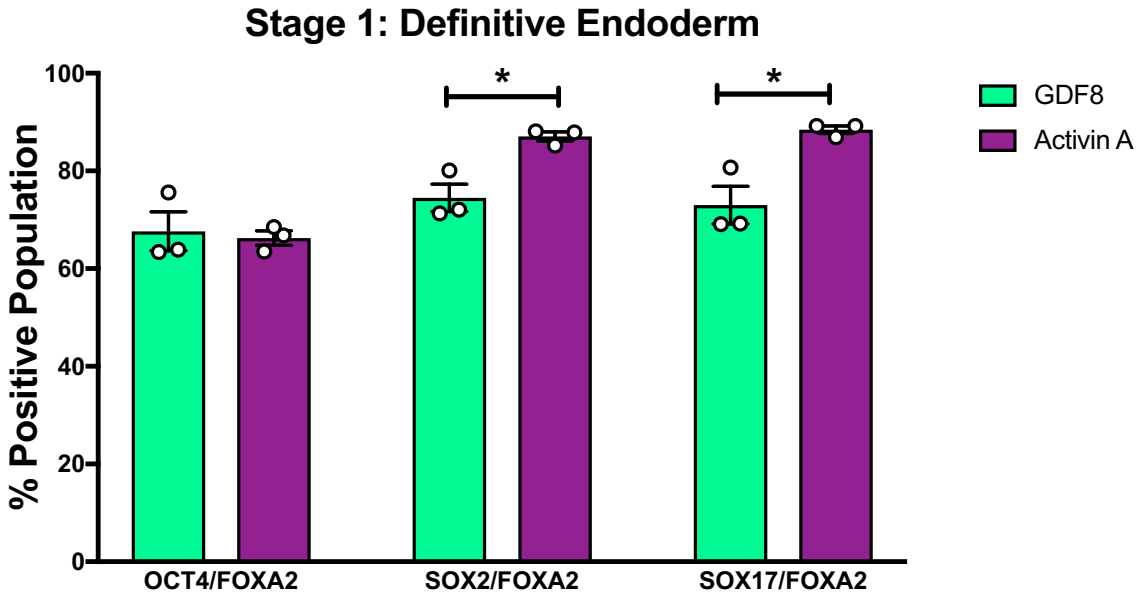

Figure 2.6 Flow cytometry analysis of Stage 1 populations of cells treated with either GDF8 or Activin A throughout Stage 1. Cells were co-stained with FOXA2 and OCT4, SOX2, or SOX17 antibodies. *P<0.05 as determined by unpaired t-test.

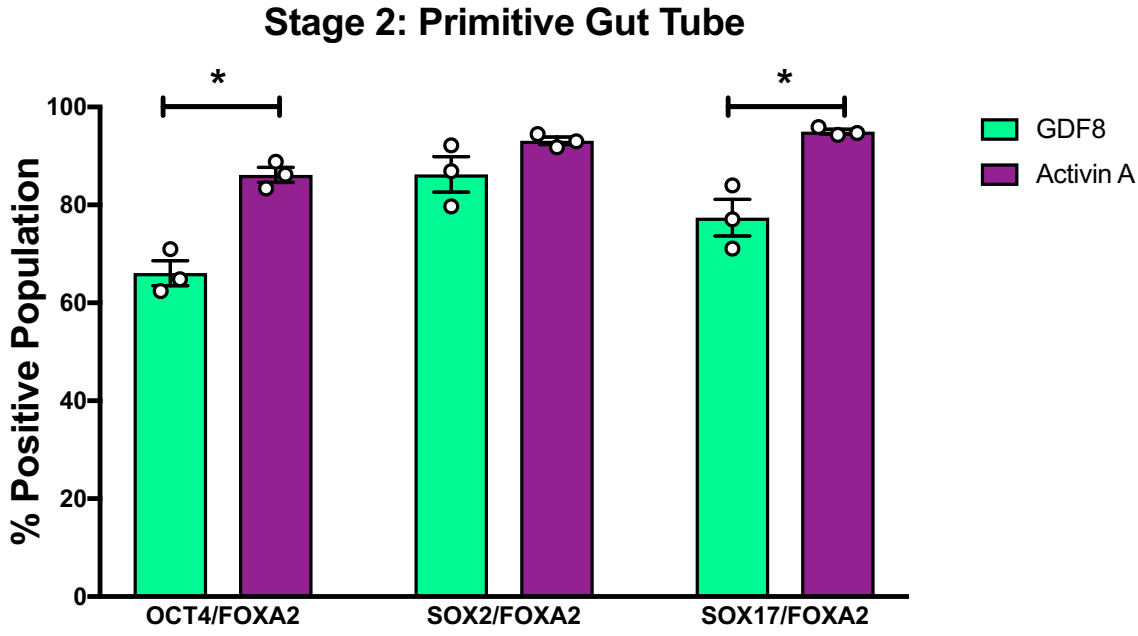

Figure 2.7 Flow cytometry analysis of Stage 2 populations of cells treated with either GDF8 or Activin A throughout Stage 1. Cells were co-stained with FOXA2 and OCT4, SOX2, or SOX17 antibodies. *P<0.05 as determined by unpaired T-test.

S3 populations contained ~80% PDX1+ cells in the Activin A treated cells compared to ~50% PDX1+ cells in the samples treated with GDF8 (Figure 2.8). In S4, the cells treated with Activin A continued to increase the proportion of cells expressing PDX1 (~95%) while the GDF8 treated samples increased to ~75% PDX1+ (Figure 2.8). NKX6.1 was also assessed in S4, where ~25% of the Activin A treated cells were NKX6.1+ versus only ~10% of GDF8-treated cells (Figure 2.8).

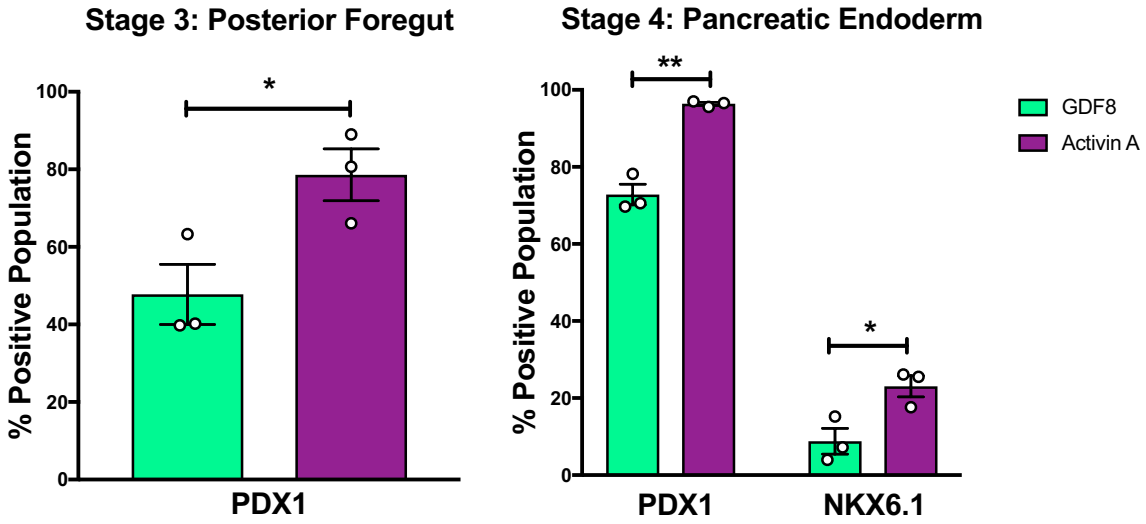

Figure 2.8 Flow cytometry analysis of S3 and S4 populations of cells treated with either GDF8 or Activin A throughout S1.Cells were stained with PDX1 and NKX6.1 antibodies. *P<0.05, **P<0.001 as determined by unpaired T-test.

The cells treated with Activin A throughout S1 differentiated with higher efficiency to S4 compared to those treated with GDF8. Activin A should therefore be used in S1 to activate the Wnt signalling pathway to ensure downstream populations (S4 and beyond) are successful and informative for screening dioxins and dioxin-like compounds.

2.4 Conclusions and Future Directions

Much of the stem cell differentiation troubleshooting for Stages 1 through 4 has been completed and the Bruin Lab can now move forward with the Rezania *et al*., 2014 protocol as a model of human beta cell differentiation. I have not yet attempted differentiating past Stage 4, however this is a clear next step for the lab once I can consistently differentiate to Stage 4 with acceptable efficiency. I will be continuing my work in the Bruin Lab as we transition my project to the next student and ensuring the protocols are complete and optimized. Several other setbacks and additional troubleshooting have happened that I have not described in detail in this chapter, but I am now familiar with the level of meticulous details required of stem cell differentiation.

3 TCDD and human beta cell development

3.1 Using hESCs as a model of human pancreas development

Human embryonic stem cells are a powerful biological tool for answering questions about human development as they have the potential to become any cell in the human body when given the appropriate environment. In **Chapter 2** I introduced hESCs and outlined the process of setting up the Bruin Lab stem cell facility and the troubleshooting involved in stem cell differentiation. In this chapter I discuss how I implemented stem cell differentiation to study the potential impact of TCDD on pancreatic beta cell development. Here, I used the STEMCELL Technologies Pancreatic Progenitor kit to differentiate hESCs toward the pancreatic lineage with higher efficiency while I continued to optimize the Rezania *et al*., 2014 protocol. The primary goal of this chapter is to explore the impact of TCDD on human pancreatic beta cell development *in vitro* using hESCs. Progress toward this goal is ongoing as I continue to answer additional questions that I did not have time to include in my MSc Thesis.

3.2 Methods

Cell culture and seeding for differentiation

hESCs (H1) were cultured and seeded for differentiation as previously described in **Chapter 2** but at 625,000 cells/well. Differentiation was initiated 24 hours post-seeding as per kit protocol.

Treatment Protocol (Pancreatic Progenitor Kit)

Differentiation with the STEMCELL Technologies STEMDiff Pancreatic Progenitor kit (#05120, STEMCELL Technologies) was implemented according to the manufacturer's published protocol. In addition to the required supplements, DMSO vehicle control or 10 nM TCDD were included daily as part of the differentiation protocol. Table 3.1 outlines the 14-day treatment and collection schedule.

Table 3.1 STEMdiff Pancreatic Progenitor kit differentiation timeline and supplements.

Day	Stage/Day	Additives	Collection
1	S1 D1	Supp. MR* CJ* DMSO or TCDD	
2	S1 D2	Supp. CJ DMSO or TCDD	
3	S2 D1	Supp. 2A Supp. 2B DMSO or TCDD	RNA Flow cytometry
4	S2 D2	Supp. 2B DMSO or TCDD	
5	S2 D3	Supp. 2B DMSO or TCDD	
6	S3 D1	Supp. 3 DMSO or TCDD	RNA Flow cytometry
7	S3 D2	Supp. 3 DMSO or TCDD	
8	S3 D3	Supp. 3 DMSO or TCDD	
9	S4 D1	Supp. 4 DMSO or TCDD	RNA Flow cytometry
10	S4 D2	Supp. 4 DMSO or TCDD	
11	S4 D3	Supp. 4 DMSO or TCDD	
12	S4 D4	Supp. 4 DMSO or TCDD	
13	S4 D5	Supp. 4 DMSO or TCDD	

14			RNA Flow cytometry

*Supplements MR and CJ are part of the STEMDiff kit and are not defined by the manufacturer.

Flow cytometry analysis

On collection days, the cells were collected and flow cytometry analysis was performed as described in **Chapter 2.** OCT4, SOX2, SOX17, and FOXA2 antibodies were used for S1 and S2, a PDX1 antibody was used in S3 and S4, and an NKX6.1 antibody was used in S4 (see Table 2.2 for dilution details).

Gene expression (RT-qPCR)

On collection days, RNA was harvested from the samples for RT-qPCR analysis of gene expression, as described in **Chapter 1**. Table 3.2 outlines the target genes and primer sequences used.

Table 3.2 Primer sequences used for gene expression analysis of differentiated cells.

Gene	Stage/Role	Forward	Reverse
OCT4	S0/Pluripotency	TGGGCTCGAGAAGGATGTG	GCATAGTCGCTGCTTGATCG
SOX2	S0/Pluripotency	GGGAAATGGGAGGGGTGCAAAAGAGG	TTGCGTGAGTGTGGATGGGATTGGTG
CXCR4	S1	CACCGCATCTGGAGAACCA	GCCCATTTCCTCGGTGTAGTT
SOX17	S1	CAAGGGCGAGTCCCGTATC	CGACTTGCCCAGCATCTTGC
FOXA2	S1	GCACTCGGCTTCCAGTATGC	GCGTTCATGTTGCTCACGGA
PDX1	S3, S4	CGTCCAGCTGCCTTTCCCAT	CCGTGAGATGTACTTGTTGAATAGGAACTC
NKX6.1	S4	GCCCGCCCTGGAGGGACGCA	ACGAATAGGCCAAACGAGCCC
ALB	Liver (albumin)	CTTCCTGGGCATGTTTTTGT	TGGCATAGCATTCATGAGGA
CDX1	Gut	GCGCAGAGGCCGACGCCCTACGAGT	TGTTCACTTTGCGCTCCTTTGCCC
CYP1A1	AhR pathway	GAACAAACAGGGCTGCCTTCT	GAGACCAATAGAAGGTAATTGAAATACCCC
AHR	AhR pathway	GTGCTTCATATGTCGTCTAAG	AATGAGTTCACATCCTGAGGC
ARNT	AhR pathway	GATGCGATGATGACCAGATGTG	CAGTGAGGAAAGATGGCTTGTAGG
PPIA	Housekeeping gene	AGCTCTGAGCACTGGAGAGA	GCCAGGACCTGTATGCTTTA

Statistics

Statistical analyses were completed using GraphPad Prism 7 software. All data are presented as mean ± SEM with individual technical replicates shown. Specific statistical tests are indicated in the legend of each figure.

3.3 Results

Flow cytometry analysis of two independent differentiations revealed appropriate changes in key markers of development (OCT4, SOX2, SOX17, FOXA2) in S1, with no apparent effect of TCDD (Figure 3.1). Analysis of S2 revealed a marked decrease in SOX2+ cells in the control samples (~60%) compared to S1, while the TCDD-treated cells maintained a high SOX2+ population (~80%) in Differentiation #1 (Figure 3.2). SOX2 is a marker of pluripotency that normally starts to decrease as cells acquire definitive endoderm identity. No significant differences were seen in either OCT4 (marker of pluripotency) or SOX17 (marker of definitive endoderm) between control and TCDD-exposed cells in S2. Unfortunately the S2 control samples from Differentiation #2 had very few viable cells after processing and therefore needs to be repeated.

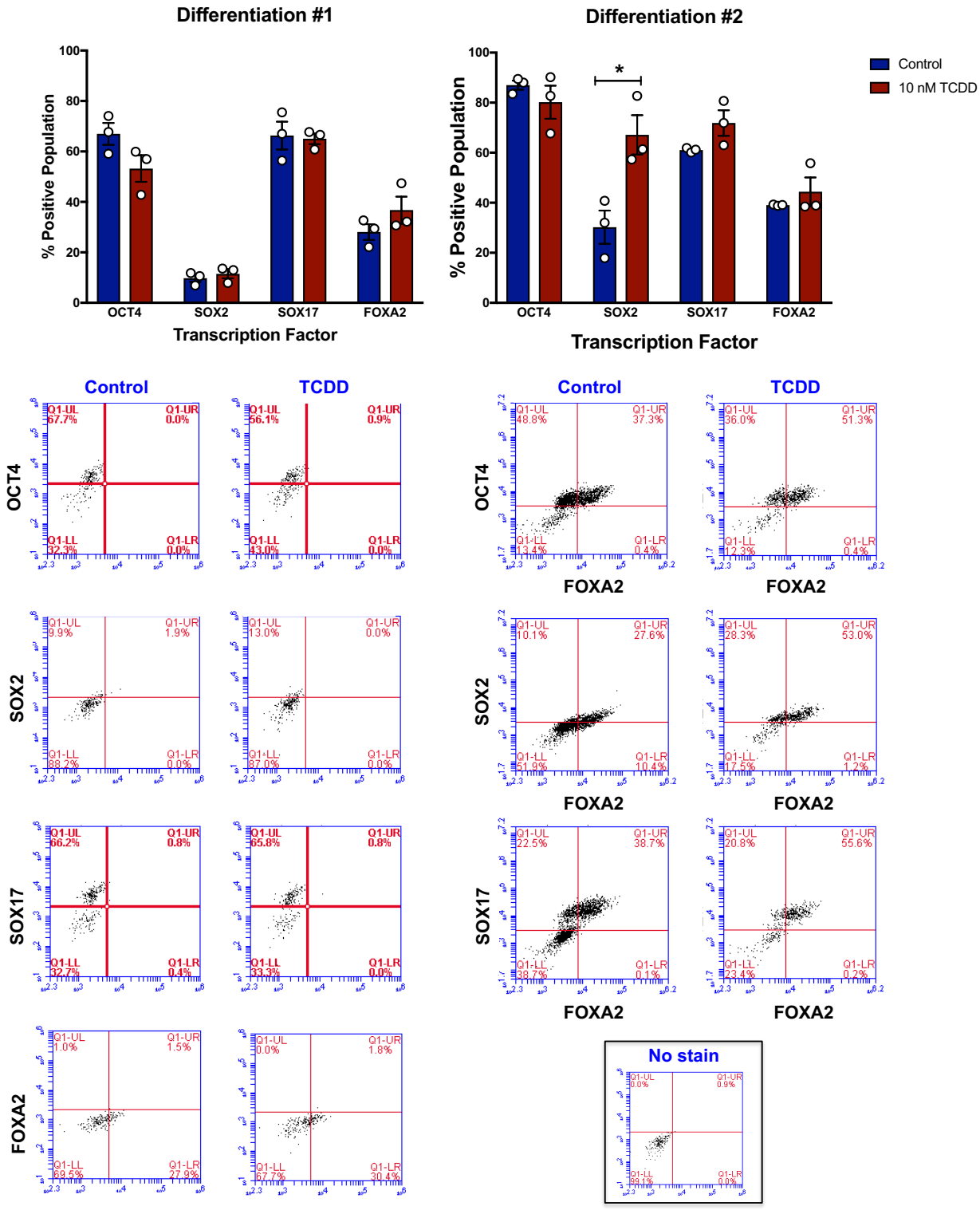

Figure 3.1 FACS analysis of S1 populations in two independent differentiations. Representative FACS plots are shown. FOXA2 was quantified in Differentiation #2 from SOX17/FOXA2 plot. T-test performed (N=3).

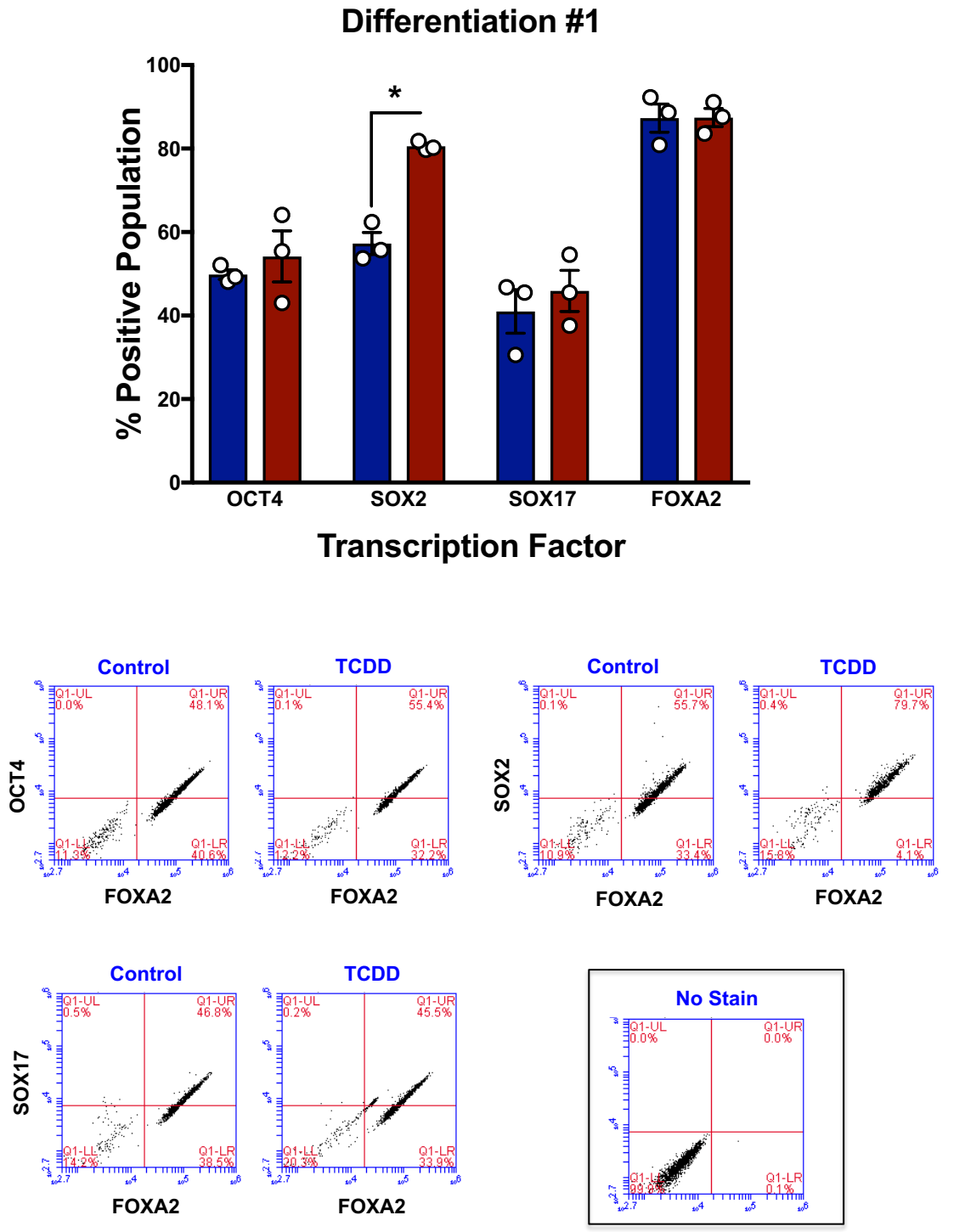

Figure 3.2 FACS analysis of S2 populations in Differentiation #1. Quantification graphs are not included for Differentiation #2 due to unreliable control samples with very few cells. FOXA2 was quantified from SOX17/FOXA2 plot. *P<0.05 as determined by T-test (N=3).

The efficiency of S3 was analyzed in terms of PDX1+ cell populations in the two independent differentiations. The control cells in both differentiations had 80-95% PDX1+ cells at the end of S3, while the TCDD-treated cells in Differentiation #1 had ~30% PDX1+ and ~80% in Differentiation #2 (Figure 3.3). Important to note, the number of analyzed TCDD-treated cells in Differentiation #1 was quite low (Figure 3.3). Differentiation #2 had a sufficient number of analyzed cells and showed no significant difference between the control and TCDD-treated cells (Figure 3.3).

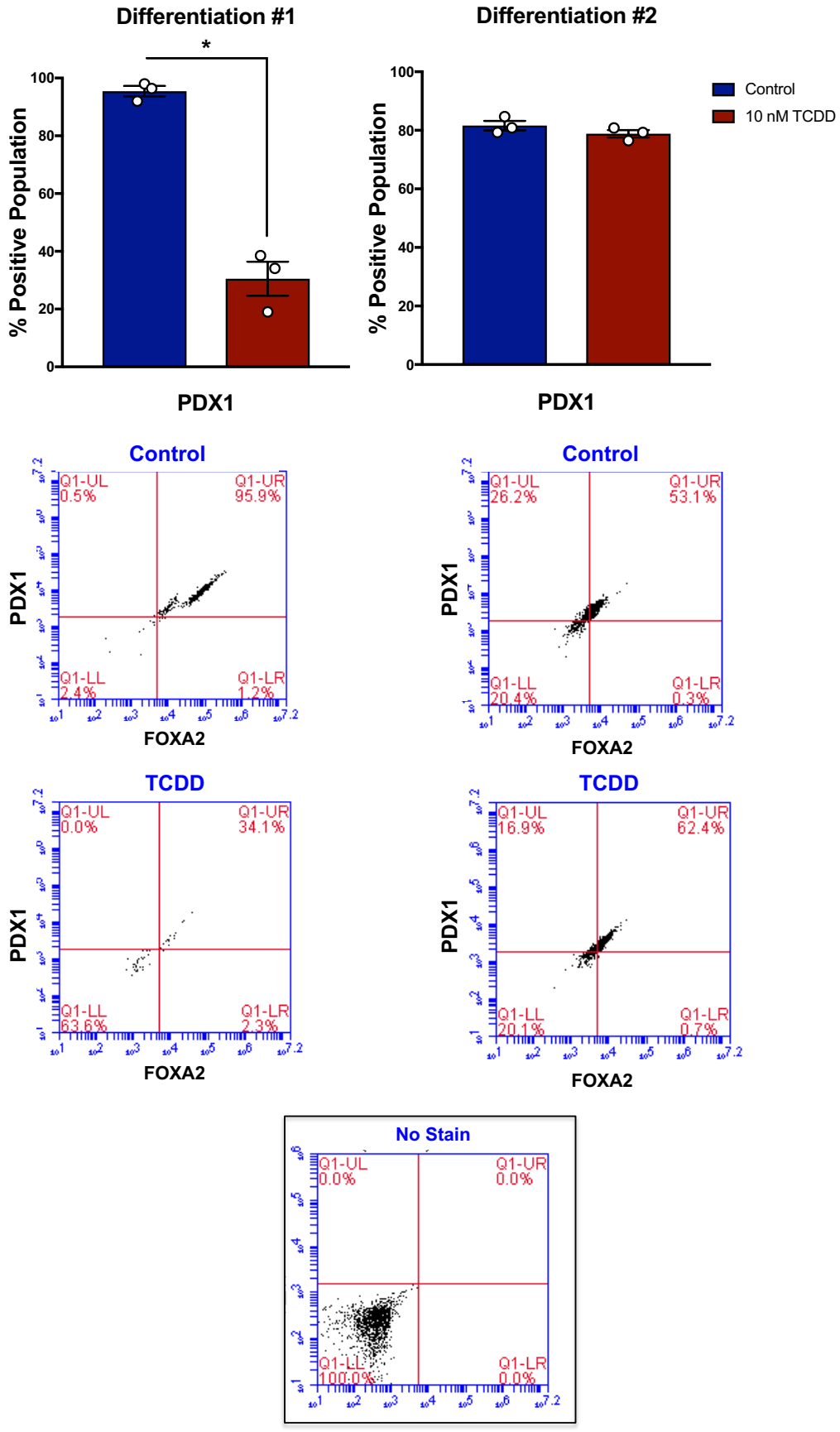

Figure 3.3 FACS analysis of S3 populations of two independent differentiations with representative FACS plots below each differentiation. Representative PDX1 plots are shown to the right. *P<0.05 as determined by T-test (N=3).

The S4D14 samples (end of S4) were analyzed for PDX1 and NKX6.1 co-expression, which is characteristic of pancreatic endoderm. Similar to the S3 plots in Figure 3.3, the TCDD-treated samples in Differentiation #1 had a low and therefore unreliable sample size due to cell death during processing (Figure 3.4). Despite this, the TCDD-treated cells had lower PDX1+ and NKX6.1+ populations (both were ~20%) compared to control (~40% and ~65%, respectively) (Figure 3.4). In Differentiation #2 no significant differences in PDX1+ and NKX6.1+ populations were found between control and TCDD-treated samples (note that control N=2 due to sample loss). Approximately 45-50% of cells were PDX1+ and 15-20% of cells were NKX6.1+ in both control and TCDD-treated samples (Figure 3.4). In an efficient differentiation, I expect that ~90% of cells should be PDX1+, while ~60% of cells should be NKX6.1+ at S4.

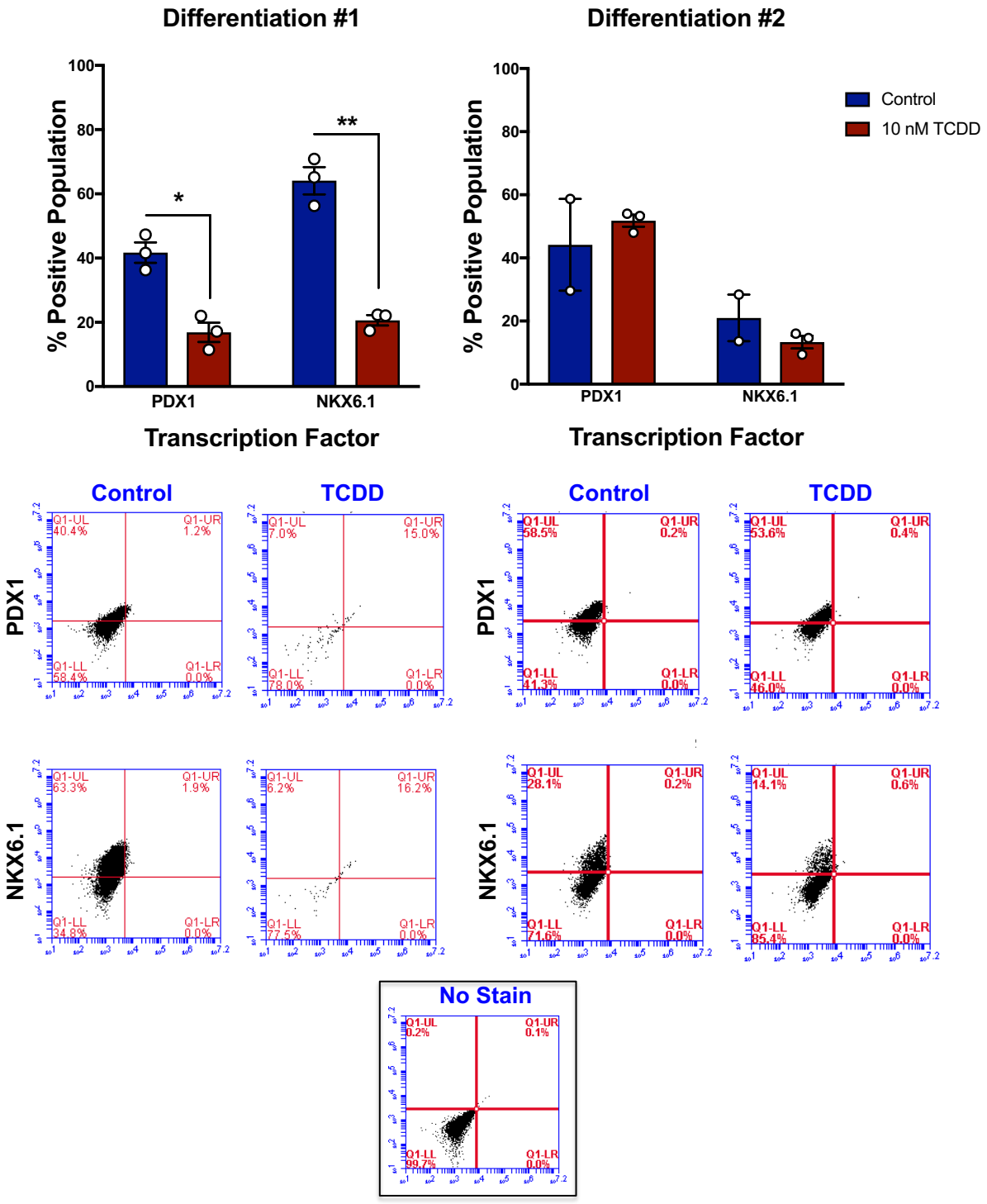

Figure 3.4 FACS analysis of S4 populations of two independent differentiations with representative FACS plots below each differentiation. *P<0.05 and **P<0.005 as determined by T-test (N=3).

RNA was isolated from each stage of Differentiation #2 to measure gene expression of the key developmental markers. Sample size varied due to the quantity of RNA isolated from each sample; where RNA concentration was too low, cDNA could not be synthesized, thus an N < 3 was used for some sample groups. I used hESCs (S0) as a control to show changes in gene expression throughout the differentiation compared to pluripotent cells. As expected, expression of pluripotency markers (*OCT4* and *SOX2*) decreased in S1 and was largely non-detectable in later stages of differentiation (Figure 3.5). TCDD did not impact expression of *OCT4* or *SOX2* compared to control.

Analysis of three markers of definitive endoderm (*CXCR4, SOX17,* and *FOXA2*) revealed appropriate increases in gene expression during S1 and S2 followed by a marked decrease, particularly of *CXCR4* and *SOX17*, in S3 and S4 (Figure 3.5). TCDD did not significantly change expression of these genes at any stage of differentiation compared to control.

Gene expression analysis of *PDX1* and *NKX6.1*, markers of S3 and S4, respectively, showed a clear increase in *PDX1* in both S3 (~50,000-fold) and S4 (~100,000-fold) as expected, in control and TCDD-treated cells (Figure 3.5). Co-expression of *PDX1* and *NKX6.1* is key for pancreatic endoderm (S4) identity. Here, *PDX1* was up-regulated in both S3 and S4, however *NKX6.1* expression was widely varied in the control group and increased only ~30-fold in the TCDD-treated cells (Figure 3.5).

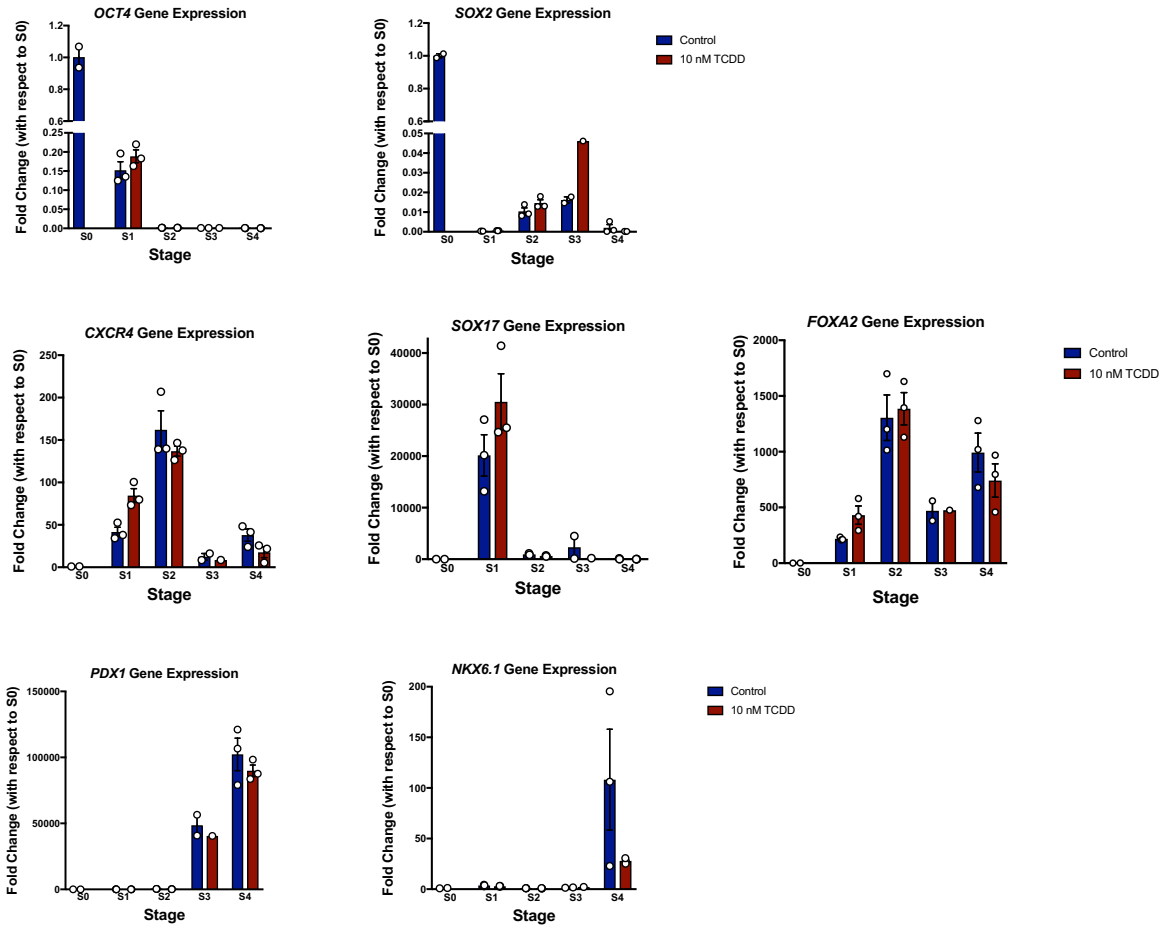

Figure 3.5 Gene expression analysis of key markers of development in Differentiation #2, normalized to H1 cells ('S0') in each stage of differentiation. T-tests performed where N=3.

I next analyzed the samples for *CYP1A1* gene expression to determine if the AhR pathway is active in early development. *CYP1A1* gene expression was increased ~8-fold in TCDD-treated cells at S2, ~160-fold by S3 (N=1) and was dramatically increased ~4500-fold compared to ~15-fold in control by S4 (Figure 3.6). Expression of *AHR* and *ARNT* could not be analyzed as I have yet to find human primers that work with these targets.

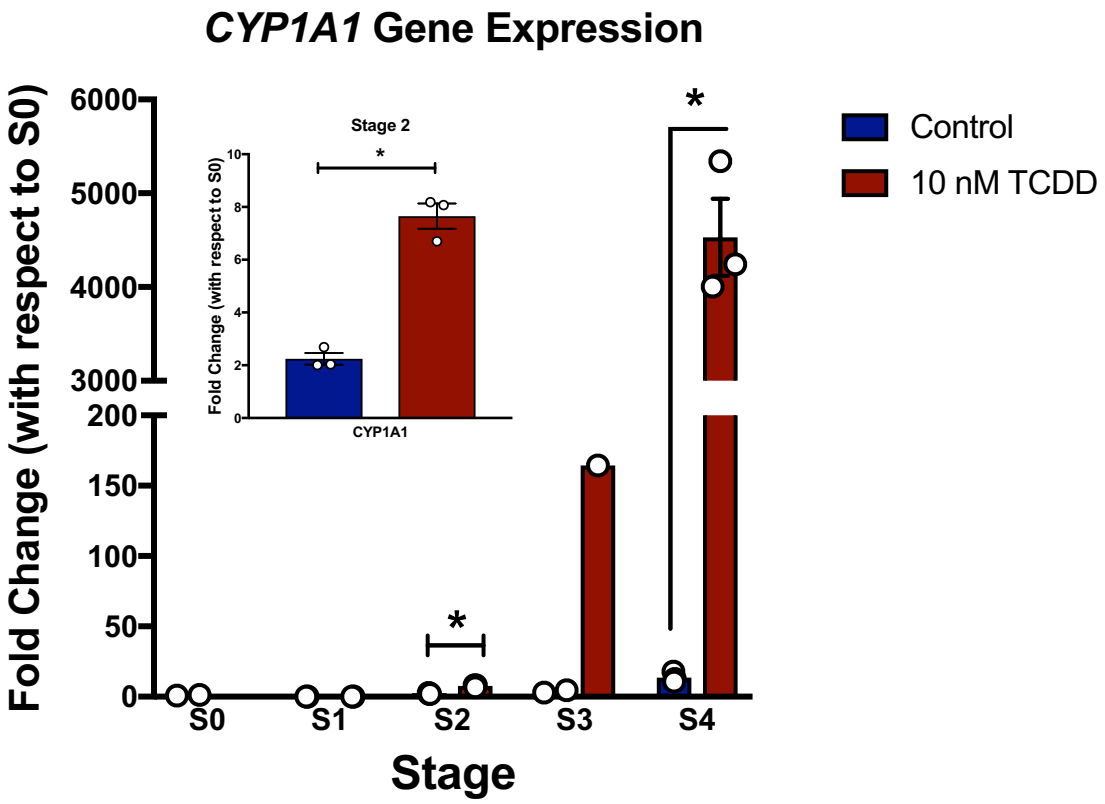

Figure 3.6 Gene expression analysis of *CYP1A1* normalized to H1 cells ('S0') in each stage of differentiation. *P<0.05 as determined by T-test (where N=3).

Gene expression of other lineage markers was analyzed to determine if a proportion of S4 cells had acquired another identity. Gene expression analysis of *ALB* (liver) and *CDX1* (gut) revealed distinct increases in TCDD-treated cells at S4 compared to control (Figure 3.7). *ALB* expression was increased ~100-fold in the control cells at S4 and ~1400-fold in TCDD-treated cells at S4. *CDX1* expression increased ~5-fold increase in the control cells compared to a ~45-fold increase in the TCDD-treated cells at S4 (Figure 3.7).

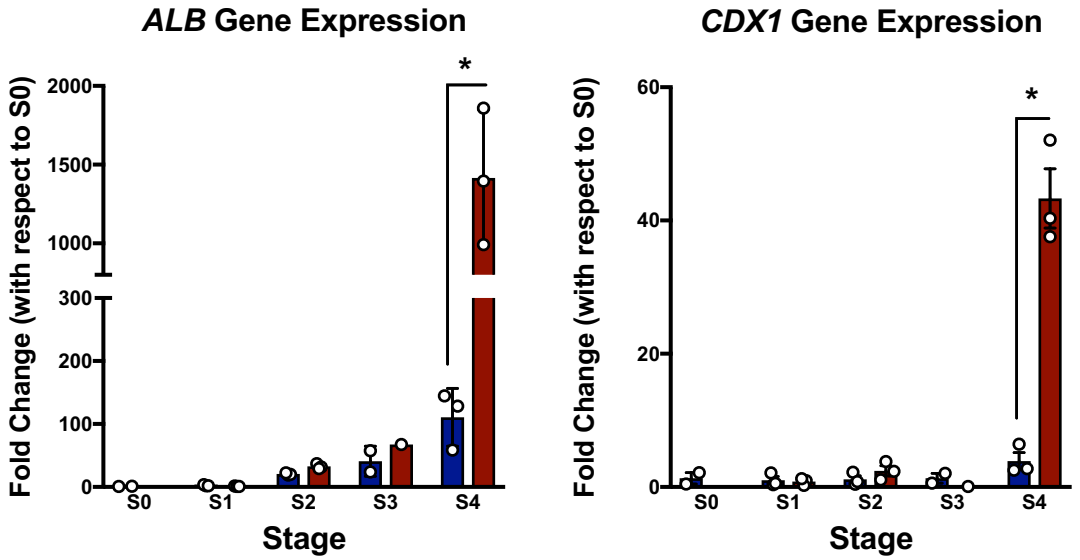

Figure 3.7 Gene expression analysis of *ALB* (liver) and *CDX1* (gut) in each stage of differentiation. *P<0.05 as determined by T-test (where N=3).

Figure 3.8 depicts representative images from Differentiation #1 taken using a light microscope. Morphological differences were apparent starting in S2 and continued to become more pronounced through to S4. The TCDD-treated cell populations were morphologically heterogeneous compared to control cells, which appeared homogenous and confluent. Figure 3.9 depicts representative images from Differentiation #2. Here, morphological differences were not as distinct as Differentiation #1 but at S4 the TCDD-treated cells appeared more heterogeneous than the control cells. In particular, the TCDD-treated cells acquired a widened, 'flat' morphology similar to those at S4 in Differentiation #1.

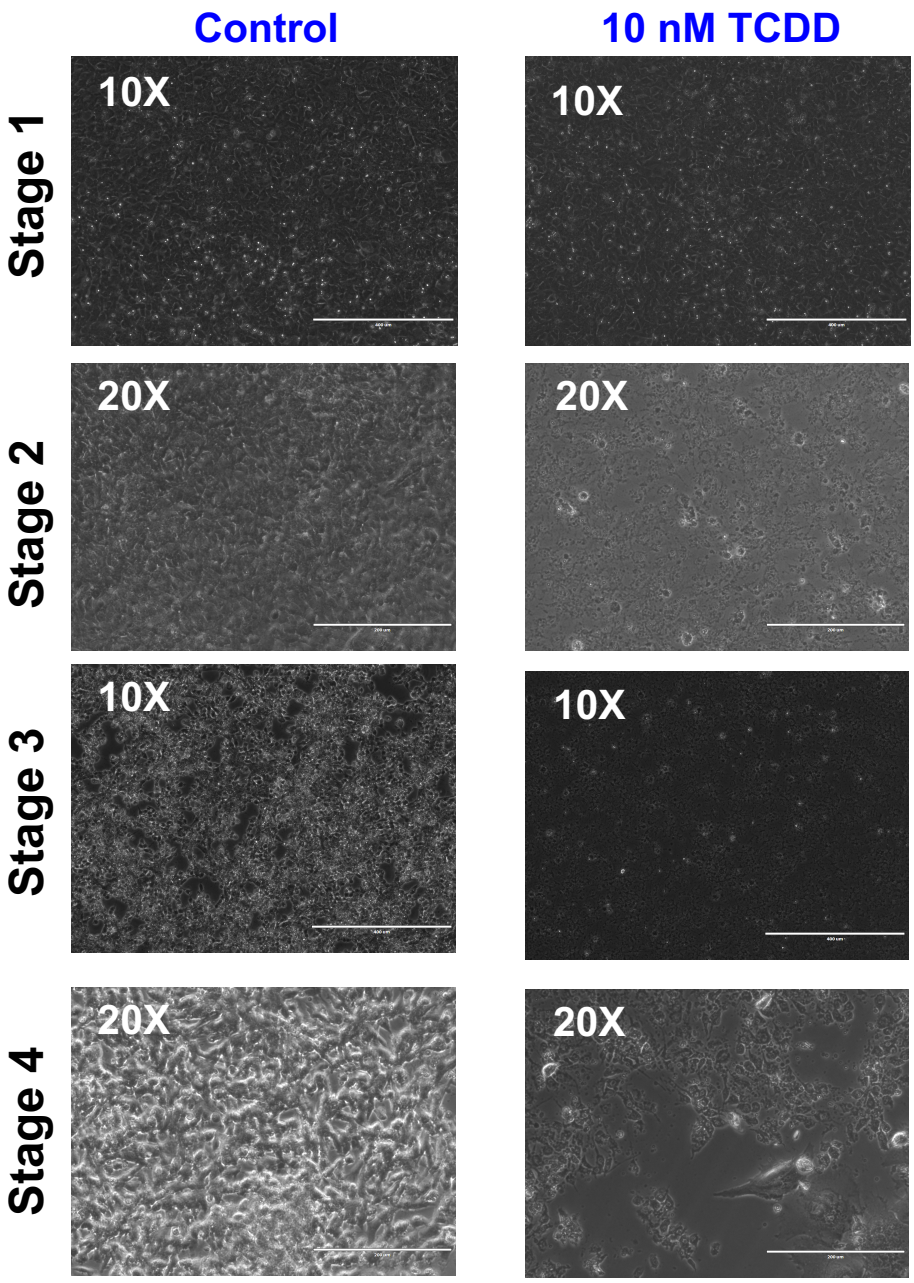

Figure 3.8 Images from S1-S4 from Differentiation #1 taken with EVOS FL light microscope. Scale bars represent 400 µm (10X) and 200 µm (20X).

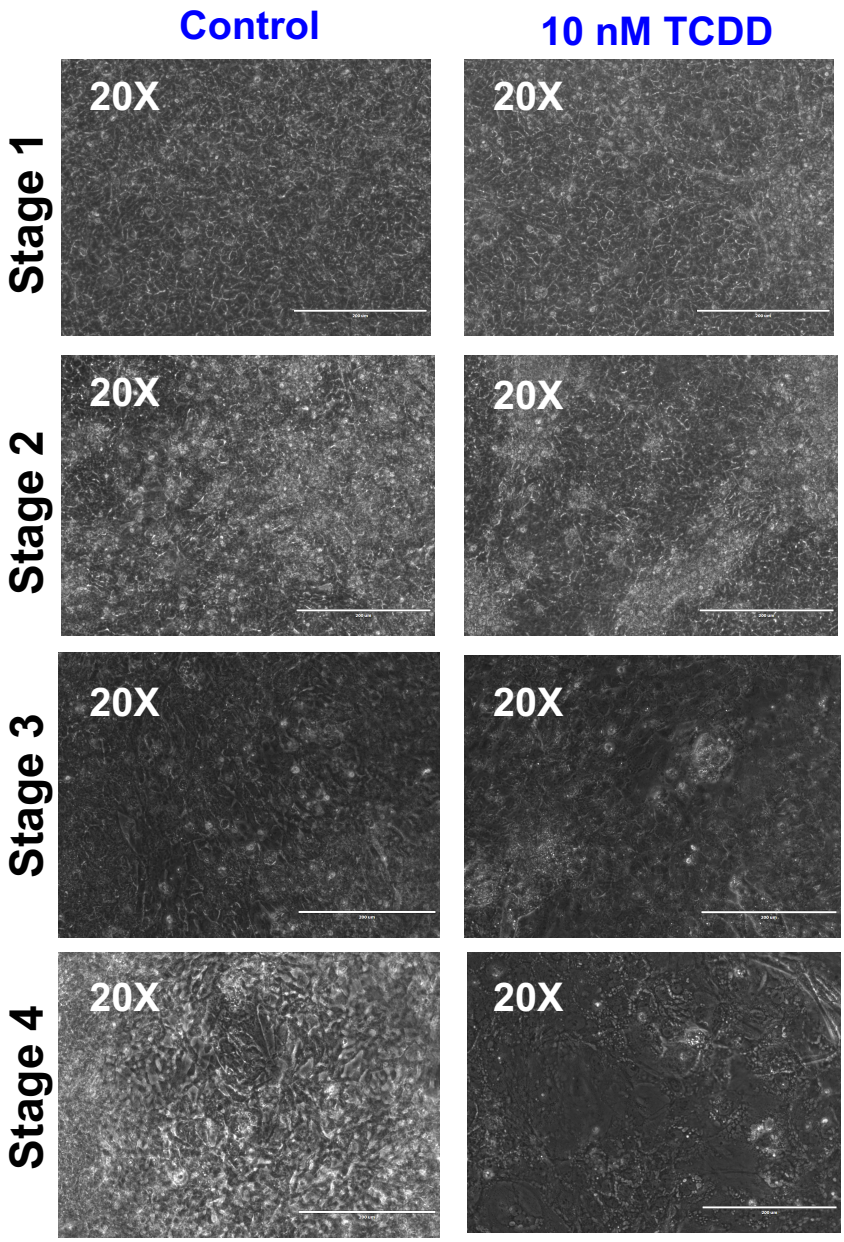

Figure 3.9 Images from S1-S4 in Differentiation #2 taken with EVOS FL light microscope. Scale bars represent 200 μm (20X).

3.4 Discussion

In this chapter I differentiated hESCs toward the pancreatic cell lineage using the STEMCELL Technologies pancreatic progenitor kit. The goal was to investigate how constant, high dose (10 nM) TCDD impacts differentiation at each stage. Here, I compare the efficiencies of two independent differentiations using flow cytometry in addition to PCR analysis of gene expression in Differentiation #2.

Flow cytometry analysis of pluripotency markers (OCT4 and SOX2) and S1 markers (SOX17 and FOXA2) revealed that constant 10 nM TCDD exposure did not change S1 efficiency in two independent differentiations. Interestingly, at S2 a significant difference in SOX2 expression was seen in Differentiation #1, wherein the TCDD-treated group had a seemingly prolonged elevation of SOX2 expression compared to control. In development, OCT4 partners with SOX2 to establish pluripotency of embryonic stem cells and as cells acquire endoderm identity OCT4 interacts with the SOX17 promoter (Aksoy *et al*., 2013; Stefanovic *et al*., 2009). This key interchange might provide an indication of early changes in differentiation occurring following TCDD exposure. Prolonged SOX2 expression could hinder efficient SOX17 expression and therefore acquisition of definitive endoderm patterning in the cells. Unfortunately, due to poor control sample quality (low cell counts) at S2 in Differentiation #2 it is not possible to make a definitive comparison to Differentiation #1. However, PCR analysis of Differentiation #2 revealed that TCDD did not significantly alter expression of any

key markers of development in S1-S4. This means that the two differentiations could be displaying different trends.

Further analysis of S3 and S4 markers in both differentiations again shows two different outcomes. In Differentiation #1 there was a marked decrease in both PDX1+ and NKX6.1+ cells in S3 and S4, however the TCDD-treated samples had a low cell count. Upon visual examination, the TCDD-treated cells were not all dying during differentiation but their physical characteristics were vastly different than in the control cells. The TCDD-treated populations became morphologically heterogeneous and were difficult to lift off the plate at S2, which could explain the low cell count in S2 and beyond. It is therefore possible that the apparent reduction in PDX1+/NKX6.1+ cells was due to an overall low cell count rather than direct effects of TCDD on markers of development. In Differentiation #2 there was no significant difference in PDX1+ or NKX6.1+ cells in S3/S4. Particular care was taken to ensure all cells had been lifted in this differentiation to ensure adequate cells for flow cytometry analysis. This experiment will have to be repeated several more times for more conclusive results.

CYP1A1 expression was analyzed in each stage of Differentiation #2. Interestingly, there was a significant increase in *CYP1A1* at S2 (primitive gut tube), a possibly (N=1) higher increase at S3 (posterior foregut), and a clear, dramatic increase at S4 (pancreatic endoderm) in the TCDD-treated cells compared to control. This marked increase in *CYP1A1* at S4 is exciting because it means that the AhR pathway is inducible early in embryonic development. Analyses of *ALB* and *CDX1*, markers of liver and gut respectively, were

performed to determine which lineage(s) a portion of the TCDD-treated cells are diverting toward. Pancreas, stomach, and liver cells arise from the foregut during embryonic development. The stomach and pancreas both develop from the posterior aspect while the liver emerges from the anterior aspect of the foregut (McCracken and Wells, 2017; Gordillo *et al*., 2015; Severn, 1971).

Interestingly, significant increases were found in both of these lineage markers at S4, which correspond to the aberrant flow cytometry data and increase in *CYP1A1*. The ~1500-fold increase in *ALB* expression in the S4 TCDD-treated cells suggests the cells are acquiring liver identity. Liver cells are well known to respond to TCDD via the AhR pathway and produce CYP1A enzymes, as the liver is the primary site for xenobiotic metabolism (Lerapetritou *et al*., 2009). Various CYP enzymes are inducible or present in the pancreas, suggesting its role as a xenobiotic-responsive organ, though literature on pancreatic CYP1A1 activity is limited (Standop *et al*., 2002; Wacke *et al*., 1998). Cell-specific AhR signalling is important for normal liver development to ensure the cells are equipped to respond to toxins, however in the context of pancreas development this effect is not well established (Walisser *et al*., 2005). Taken together, these preliminary data presented here suggest that TCDD is interfering with appropriate developmental pathways *in vitro*, potentially through the activation of the AhR pathway and subsequent transcription of *CYP1A1*. Further experimentation is required to confirm and reproduce these initial findings.

3.5 Conclusions and Future Directions

In this chapter I generated a preliminary set of data suggesting that TCDD is impacting normal pancreatic development *in vitro*, though the mechanism has not yet been elucidated. Specifically, I showed that TCDD promotes a greater subset of cells to differentiate into other lineages (liver, gut) compared to a normal differentiation. I also found that *CYP1A1* expression is increased modestly in S2 and dramatically in S4, which means the AhR pathway is active as early as 'primitive gut tube'. Whether the increase in *CYP1A1* is due to the induction of other lineages, is present in the developing pancreas, or both, remains to be discovered. In the context of human pancreatic beta cell development, the presence of TCDD or other dioxin-like chemicals in the embryo's environment may interfere with the generation of a healthy beta cell population.

In Chapter 1 I addressed the need for human *AhR* and *ARNT* primers, which would be useful here to identify at which point the AhR machinery is present in pancreatic development. It would also be informative to start co-staining PDX1 and NKX6.1 for flow cytometry analysis, as this would provide more insight into the cell populations present at S3 and S4. I would also like to perform a CYP1A1 enzyme activity assay in parallel to HepG2 cells to determine if the increase in gene expression correlates to functional enzymes. As mentioned in the discussion, I plan to repeat this experiment but with a greater number of technical and biological replicates. Further, I will implement the

Rezania *et al*., 2014 protocol to investigate whether the effects seen here are reproducible with a different differentiation regimen.

Conclusions and Final Thoughts

The primary goal of this thesis was to investigate the impact of TCDD on human and rodent pancreatic beta cell development and physiology, respectively. A second but equally important goal was to establish the Bruin Lab tissue culture facility and implement hESC differentiation protocols.

In Chapter 1 I concluded that the rodent endocrine lines studied are not appropriate models of human alpha or beta cell physiology for the purpose of studying responses to pollutants that act via AhR. The INS-1 cells were the only rodent cell line to show a modest response to TCDD in terms of *Cyp1a1* gene expression. These cells also had higher overall insulin content when treated with 1 nM or 10 nM TCDD for 48 hours compared to control. Increased *Cyp1a1* may change beta cell physiology, perhaps resulting in increased insulin content and leading to eventual beta cell exhaustion and dysfunction. Two possible mechanisms for this include increased calcium influx (Kim *et al*., 2009) or through ROS damage within the beta cell, or more specifically the mitochondria. Mitochondrial stress and damage could result in changes in insulin synthesis and secretion, as it is a central player in glucose metabolism. Insulin secretion was not assessed in other rodent cell lines, so it remains unclear if the modest increase in *Cyp1a1* gene expression is specifically linked to the increase in insulin content seen in the INS-1 cells.

In Chapter 2 I explained some of the key troubleshooting I conducted and discussed current progress toward this goal. For example, I established optimal seeding densities and additive concentrations required for efficient S1

differentiation in our hands, as well as overall workflow. I learned that stem cell culture and differentiation requires a much higher level of planning and attention to detail than basic tissue culture with immortalized cell lines. This aspect of my project required the most time and effort of all three chapters, such that the stem cell differentiation experiments discussed in Chapter 3 only occurred in the last few months due to the extent of optimization and learning that had to be done. I also went to the Kieffer Lab at the University of British Columbia for one week to get additional hands-on training with their stem cell specialist. In the coming months I will continue to hone these protocols and train new members of the Bruin Lab in tissue culture.

In Chapter 3 I explored the impact of continuous TCDD exposure on differentiation toward the pancreatic lineage and discovered that TCDD was diverting a subset of the cell population toward liver and gut fates. I also found a modest increase in *CYP1A1* expression in S2 and a pronounced increase by S4. This marked increase was not seen in any of the rodent cell lines, perhaps because the rodent lines have been derived from tumours or transfected with SV40 virus, rendering the lines immortal *in vitro*, and changing their physiology.

Taken together, the data suggest that exposure to dioxins and dioxin-like compounds during embryonic development could impede appropriate tissue development. Proper fetal development of pancreatic beta cells is particularly important because they have a very limited proliferative capacity, unlike closely related liver cells. Therefore, if dioxin-like compounds are changing the developmental environment through induction of *CYP1A1* or other downstream

AhR targets, it is possible that a sufficient number of functional beta cells will not be formed, thereby predisposing an individual to metabolic challenges later in life. In a broader sense, this disruption during pancreatic development could be an avenue for the pathogenesis of diabetes, however additional experimentation is necessary to further investigate this hypothesis.

References

Aksoy I, R Jauch, J Chen, M Dyla, U Divakar, GK Bogu, R Teo, CKL Ng, W Herath, S Lili, AP Hutchins, P Robson, PR Kolatkar, and LW Stanton. Oct4 switches patterning from Sox2 to Sox17 to reinterpret the enhancer code and specify endoderm. ***The EMBO Journal***, 3(32):938-953. 2013.

Ballotari P, M Vicentini, V Manicardi, M Gallo, S Chiatamone Ranieri, M Greci, and P Giorgi Rossi. Diabetes and risk of cancer incidence: results from a population-based cohort study in northern Italy. ***BMC Cancer***, 17:703. 2017.

Bertazzi PA, I Bernucci, G Brambilla, D Consonni, and AC Pesatori. The Seveso studies on early and long-term effects of dioxin exposure: a review. ***Environmental Health Perspectives***, 106(2):625-633. 1998.

Bofinger DP, L Feng, LH Chi, J Love, FD Stephen, TR Sutter, KG Osteen, TG Costich, RE Batt, ST Koury, and JR Olson. Effect of TCDD exposure on CYP1A1 and CYP1B1 expression in explant culture of human endometrium. ***Toxicological Sciences***, 62(2):299-314. 2001.

Codru N, MJ Schymura, S Negoita, R Rej, and DO Carpenter. Diabetes in relation to serum levels of polychlorinated biphenyls and chlorinated pesticides in adult Native Americans. ***Environmental Health Perspectives***, 115(10):1442-1447. 2007.

Gordillo M, T Evans, and V Gouon-Evans. Orchestrating liver development. ***Development***, 142:2094-2108. 2015.

Henriksen GL, NS Ketchum, JE Michalek, and JA Swaby. Serum dioxin and diabetes mellitus in veterans of Operation Ranch Hand. ***Epidemiology***, 8:252-258. 1997.

Hooper K, T Chuvakova, G Kazbekova, D Hayward, A Tulenova, MX Petreas, Tk Wade, K Benedict, YY Cheng, and J Grassman. Analysis of breast milk to assess exposure to chlorinated contaminants in Kazakhstan: sources of 2,3,7,8-tetrachlorodibenzo-p-dioxin (TCDD) exposures in an agricultural region of southern Kazakhstan. ***Environmental Health Perspectives***, 107(6):447-457. 1999.

International Diabetes Foundation. IDF Diabetes Atlas. 8th edition. 2017.

Kang HK, NA Dalager, LL Needham, DG Patterson Jr, P SJ Lees, K Yates, and GM Matanoski. Health status of army chemical corps Vietnam veterans who sprayed defoliant in Vietnam. ***American Journal of Industrial Medicine***, 49:875-884. 2006.

Kim YH, YJ Shim, YJ Shin, D Sul, E Lee, and BH Min. 2,3,7,8-tetrachlorodibenzo-p-dioxin (TCDD) induces calcium influx through T-type calcium channel and enhances lysosomal exocytosis in INS-1 cells. ***International Journal of Toxicology***, 28(3):151-161. 2009.

Lee DH and HM Chung. Differentiation into endoderm lineage: pancreatic differentiation from embryonic stem cells. ***International Journal of Stem Cells***, 4(1):35-42. 2011.

Lee DH, MW Steffes, A Sjodin, RS Jones, LL Needham, and DR Jacobs Jr. Low dose of some persistent organic pollutants predicts type 2 diabetes: a nested case-control study. ***Environmental Health Perspectives***, 118(9):1235-1242. 2010.

Lerapetritou M, PG Georgopoulos, CM Roth, and LP Androulakis. Tissue-level modeling of xenobiotic metabolism in liver: an emerging tool for enabling clinical translational research. ***Clinical and Translational Science***, 2(3):228-237. 2009.

Longnecker MP and JE Michalek. Serum dioxin level in relation to diabetes mellitus among Air Force veterans with background levels of exposure. ***Epidemiology***, 11(1):44-48. 2000.

Mandl M and R Depping. Hypoxia-inducible aryl hydrocarbon receptor nuclear translocator (ARNT) (HIF-1beta): is it a rare exception? ***Molecular Medicine***, 20:215-220. 2014.

McCracken KW and JM Wells. Mechanisms of embryonic stomach development. ***Seminars in Cell and Developmental Biology***, 66:36-42. 2017.

Nau H, R Bass, and D Neubert. Transfer of 2,3,7,8-tetrachlorodibenzo-p-dioxin (TCDD) via placenta and milk, and postnatal toxicity in the mouse. ***Archives of Toxicology***, 59(1):36-40. 1986.

Naujok O, U Diekmann, and S Lenzen. The generation of definitive endoderm from human embryonic stem cells is initially independent from activin A but requires canonical Wnt-signaling. ***Stem Cell Reviews and Reports***, 10(4):480-493. 2014.

Nebert DW and TP Dalton. The role of cytochrome P450 enzymes in endogenous signaling pathways and environmental carcinogenesis. ***Nature Reviews Cancer***, 6:947-960. 2006.

Noakes R. The aryl hydrocarbon receptor: a review of its role in the physiology and pathology of the integument and its relationship to the tryptophan metabolism. ***International Journal of Tryptophan Research***, 8:7-18. 2015.

Pagliuca FW, JR Millman, M Gurtler, M Segel, A Van Dervort, J Hyoje Ryu, QP Peterson, D Greiner, and DA Melton. Generation of functional pancreatic beta cells in vitro. ***Cell***, 159:428-439. 2014.

Persky V, J Piorkowski, M Turyk, S Freels, R Chatterton Jr, J Dimos, HL Bradlow, L Kaatz Chary, V Burse, T Unterman, DW Sepkovic, and K McCann. Polychlorinated biphenyl exposure, diabetes and endogenous hormones: a cross-sectional study in men previously employed at a capacitor manufacturing plant. ***Environmental Health***, 11:57. 2012.

Piaggi S, M Novelli, L Martino, M Masini, C Raggi, E Orciuolo, R Masiello, A Casini, and V De Tata. Cell death and impairment of glucose-stimulated insulin secretion induced by 2,3,7,8-tetrachlorodibenzo-p-dioxin (TCDD) in the beta-cell line INS-1E. ***Toxicology and Applied Pharmacology***, 220(3):333-340. 2007.

Pollenz RS. The aryl-hydrocarbon receptor, but not the aryl-hydrocarbon receptor nuclear translocator protein, is rapidly depleted in hepatic and nonhepatic cultur cells exposed to 2,3,7,8-tetrachlorodibenzo-p-dioxin. ***Molecular Pharmacology***, 49(3):391-398. 1996.

Rezania A, JE Bruin, P Arora, A Rubin, I Batushansky, A Asadi, S O'Dwyer, N Quiskamp, M Mojibian, T Albrecht, YHC Yang, JD Johnson, and TJ Kieffer. Reversal of diabetes with insulin-producing cells derived *in vitro* from human pluripotent stem cells. ***Nature Biotechnology***, 32(11):1121-1133. 2014.

Rostovskaya M, N Bredenkamp, and A Smith. Towards consistent generation of pancreatic lineage progenitors from human pluripotent stem cells. ***Philosophical Transactions Royal Society Publishing B***, 370:20140365. 2015.

Ruzzin J, R Petersen, E Meugnier, L Madsen, EJ Lock, H Lillefosse, T Ma, S Pesenti, SB Sonne, TT Marstrand, MK Malde, ZY Du, C Chavey, L Fajas, AK Lundebye, CL Brand, H Vidal, K Kristiansen, and L Froyland. Persistent organic pollutant exposure leads to insulin resistance syndrome. ***Environmental Health Perspectives***, 118(4):465-471. 2010.

Schecter A, H McGee, JS Stanley, K Boggess, and P Brandt-Rauf. Dioxins and dioxin-like chemicals in blood and semen of American Vietnam veterans from the state of Michigan. ***American Journal of Industrial Medicine***, 31(3):370-371. 1996.

Severn CB. A morphological study of the development of the human liver. ***The American Journal of Anatomy***, 131(2):133-158. 1971.

Shin JS, YS Kwon, JJ Lee, and CW Kim. Isolation of ethanol-induced genes in pancreatic beta-cells by representational difference analysis (RDA). ***Experimental and Molecular Medicine***, 36(1):36-42. 2004.

Spencer DL, SA Masten, KM Lanier, X Yang, JA Grassman, CR Miller, TR Sutter, GW Lucier, and NJ Walker. Quantitative analysis of constitutive and 2,3,7,8,-tetrachlorodibenzo-p-dioxin-induced cytochrome P450 1B1 expression in human lymphocytes. ***Cancer Epidemiology, Biomarkers and Prevention***, 8:139-146. 1999.

Standop J, AB Ulrich, MB Schneider, MW Buchler, and PM Pour. Differences in the expression of xenobiotic-metabolizing enzymes between islets derived from the ventral and dorsal anlage of the pancreas. ***Pancreatology***, 2(6):510-518. 2002.

Stefanovic S, N Abboud, S Desilets, D Nury, C Cowan, and M Puceat. Interplay of Oct4 with Sox2 and Sox17: a molecular switch from stem cell pluripotency to specifying a cardiac fate. ***The Journal of Cell Biology***, 186(5):665-673. 2009.

Stejskalova L and P Pavek. The function of cytochrome P450 1A1 enzyme (CYP1A1) and aryl hydrocarbon receptor (AhR) in the placenta. ***Current Pharmaceutical Biotechnology***, 12(5):715-730. 2011.

Vogel CFA and T Haarmann-Stemmann. The aryl hydrocarbon receptor repressor – more than a simple feedback inhibitor of AhR signaling: clues for its role in inflammation and cancer. ***Current Opinion in Toxicology***, 2:190-119. 2017.

Wacke R, A Kirchner, F Prall, H Nizze, W Schmidt, U Fischer, FP Nitschke, U Adam, P Fritz, C Belloc, and B Drewelow. Up-regulation of cytochrome P450 1A2, 2C9, and 2E1 in chronic pancreatitis. ***Pancreas***, 16(4):521-528. 1998.

Walisser JA, E Glover, K Pande, AL Liss, and CA Bradfield. Aryl hydrocarbon receptor-dependent liver development and hepatotoxicity are mediated by different cell types. ***PNAS***, 102(49):17858-17863. 2005.

Wang Z, W Li, T Chen, J Yang, Z Wen, X Yan, T Shen, and R Liang. Activin A can induce definitive endoderm differentiation from human parthenogenetic embryonic stem cells. ***Biotechnology Letters***, 37:1711-1717. 2015.

Westerink WM and WG Schoonen. Cytochrome P450 enzyme levels in HepG2 cells and cryopreserved primary human hepatocytes and their induction in HepG2 cells. ***Toxicology in Vitro***, 21(8):1581-1591. 2007.

Xavier, G DS. The cells of the islets of Langerhans. ***Journal of Clinical Medicine***, 7(3):54. 2018.

Xu C, MS Inokuma, J Denham, K Golds, P Kundu, JD Gold, and MK Carpenter. Feeder-free growth of undifferentiated human embryonic stem cells. ***Nature Biotechnology***, 19(10):971-974. 2001.

Ye M, M Warner, P Mocarelli, P Brambilla, and B Eskenazi. Prenatal exposure to TCDD and atopic conditions in the Seveso second generation: a prospective cohort study. ***Environmental Health***, 17:22. 2018.

Yueh MF, M Kawahara, and J Raucy. Cell-based high-throughput bioassays to assess induction and inhibition of CYP1A enzymes. ***Toxicology in Vitro***, 19(2):275-287. 2005.

Appendix A

Table A1 Complete list of PCR primers (from Integrated DNA Technologies).

Gene	Species	Forward	Reverse
CYP1A1	Human	GAACAAACAGGGCTGCCTTCT	GAGACCAATAGAAGGTAATTGAAATACCCC
Cyp1a1	Mouse	ATCACAGACAGCCTCATTGAGC	AGATAGCAGTTGTGACTGTGTC
AhR	Human	GTGCTTCATATGTCGTCTAAG	AATGAGTTCACATCCTGAGGC
Ahr	Mouse	AGCCGGTGCAGAAAACAGTAA	AGGCGGTCTAACTCTGTGTTC
ARNT	Human	GATGCGATGATGACCAGATGTG	CAGTGAGGAAAGATGGCTTGTAGG
Arnt	Mouse	GACAGACCACAGGACAGTTCC	AGCATGGACAGCATTTCTTGAA
ALB	Human	CTTCCTGGGCATGTTTTTGT	TGGCATAGCATTCATGAGGA
CDX1	Human	GCGCAGAGGCCGACGCCCTACGAGT	TGTTCACTTTGCGCTCCTTTGCCC
NKX2.1	Human	CAGGACACCATGAGGAACAGCG	GCCATGTTCTTGCTCACGTCCC
PPIA	Human/ mouse	AGCTCTGAGCACTGGAGAGA	GCCAGGACCTGTATGCTTTA
HPRT	Human	TGTTGTAGGATATGCCCTTGACTAT	GCGATGTCAATAGGACTCCAGA
Hprt	Mouse	GCTGACCTGCTGGATTACAT	TTGGGGCTGTACTGCTTAAC
OCT4	Human	TGGGCTCGAGAAGGATGTG	GCATAGTCGCTGCTTGATCG
SOX2	Human	GGGAAATGGGAGGGGTGCAAAAGAGG	TTGCGTGAGTGTGGATGGGATTGGTG
CXCR4	Human	CACCGCATCTGGAGAACCA	GCCCATTTCCTCGGTGTAGTT
SOX17	Human	GGCGCAGCAGAATCCAGA	CCACGACTTGCCCAGCAT
FOXA2	Human	CAAGGGCGAGTCCCGTATC	CGACTTGCCCAGCATCTTGC
PDX1	Human	CGTCCAGCTGCCTTTCCCAT	CCGTGAGATGTACTTGTTGAATAGGAACTC
NKX6.1	Human	GCCCGCCCTGGAGGGACGCA	ACGAATAGGCCAAACGAGCCC